

Theoretical Study of High Temperature Superconductivity

T. Yanagisawa¹, M. Miyazaki², K. Yamaji¹

¹ National Institute of Advanced Industrial Science
and Technology (AIST)

² Hakodate National College of Technology

Outline

1. Introduction
2. Superconductivity
3. High Temperature Superconductivity
4. Hubbard Model
5. Variational Monte Carlo method
6. Stripes in high-T_c cuprates
7. Spin-orbit coupling and Lattice distortion
8. Summary

1. Introduction

Key words: Physics from U (Coulomb interactions)

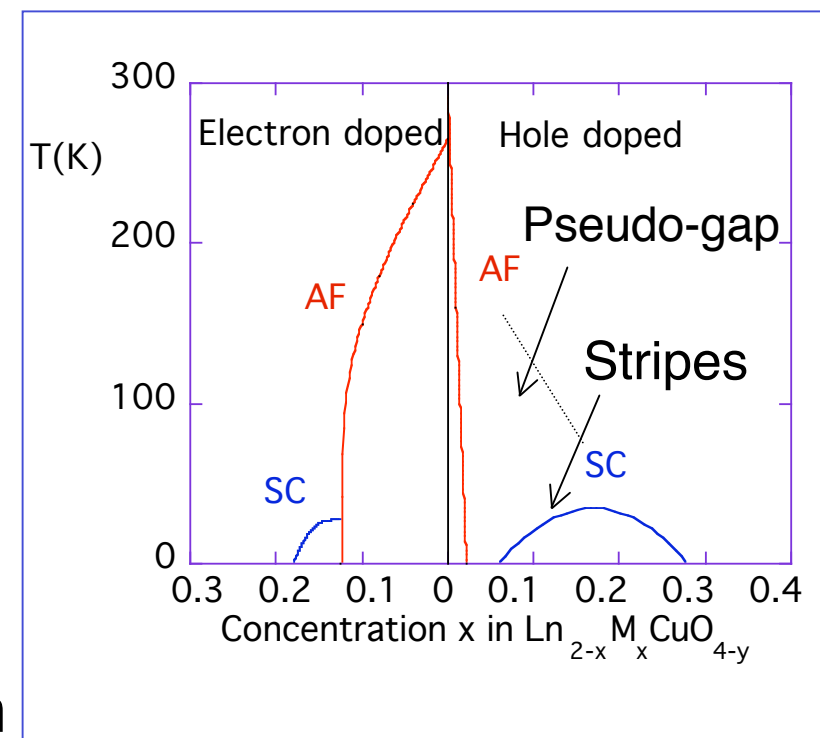
- A possibility of superconductivity
Superconductivity from U

- Competition of AF and SC

- Incommensurate state
Stripes and SC
Compete and Collaborate

- Stripes in the lightly-doped region

- Singular Spectral function



Purpose of Theoretical study

1. Origin of the superconductivity

- Symmetry of Cooper pairs
- Mechanism of attractive interaction

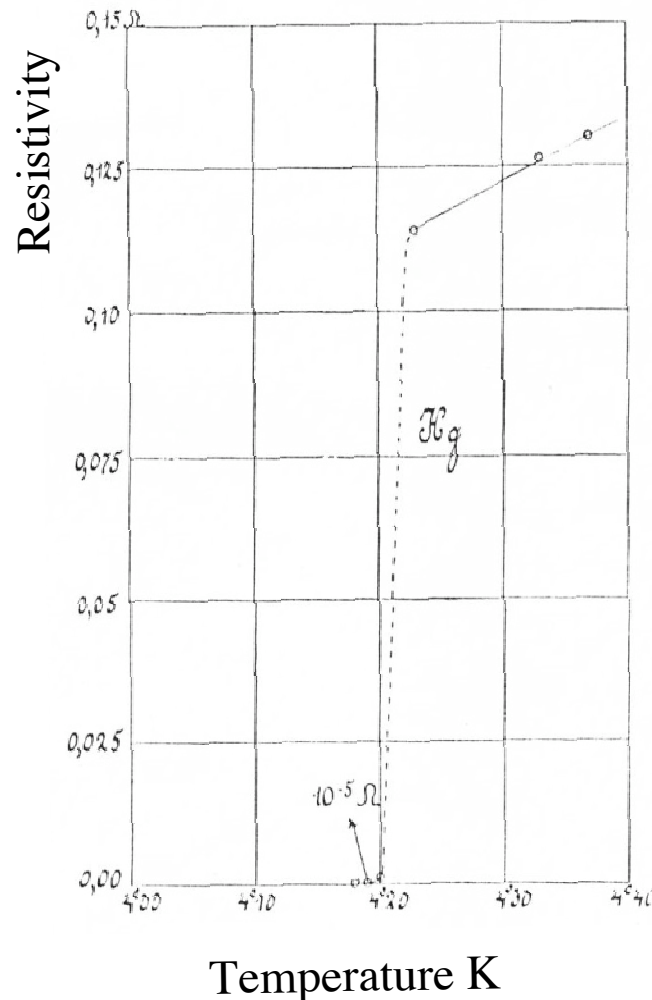
Coulomb interaction U , Exchange interaction J

2. Physics of Anomalous Metallic behavior

- Inhomogeneous electronic states: stripe
- Pseudogap phenomena
- Structural transition LTO, LTT

2. Superconductivity

1911 Kamerlingh Onnes



Elements that become superconducting

A periodic table where elements are colored based on their superconducting properties. Elements highlighted in orange are superconductive under pressure, and elements highlighted in pink are superconductive at low temperatures.

H	He																	
Li	Be																	
Na	Mg																	
K	Ca	Sc	Ti	V	Cr	Mn	Fe	Co	Ni	Cu	Zn	Ga	Ge	As	S	O	F	Ne
Rb	Sr	Y	Zr	Nb	Mo	Tc	Ru	Rh	Pd	Ag	Cd	In	Sn	Sb	Te	Br	Kr	
Cs	Ba	La	Hf	Ta	W	Re	Os	Ir	Pt	Au	Hg	Tl	Pb	Bi	Po	At	Xe	
Fr	Ra	Ac	Ru	Ha	Unh	Uns	Uno	Une									Rn	
Ce	Pr	Nd	Pm	Sm	Eu	Gd	Tb	Dy	Ho	Er	Tm	Yb	Lu					
Th	Pa	U	Np	Pu	Am	Cm	Bk	Cf	Es	Fm	Md	No	Lr					



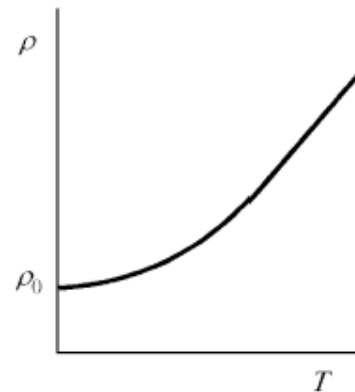
Superconductive at low temperatures



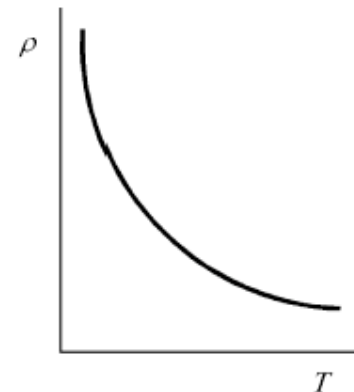
Superconductive under pressure

Characteristics of Superconductivity

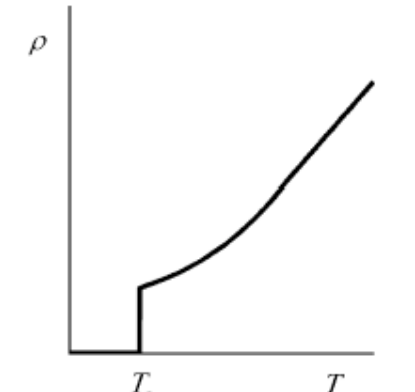
Electrical
Resistivity



Metal

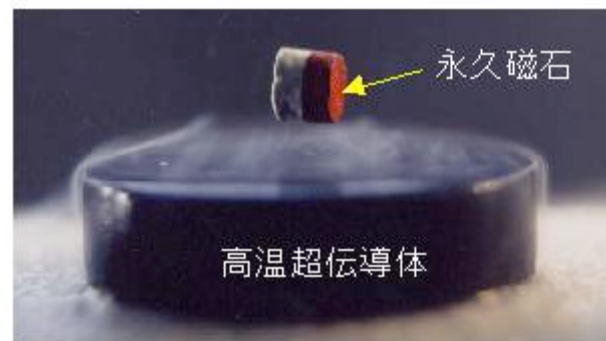


Semiconductor



Superconductor

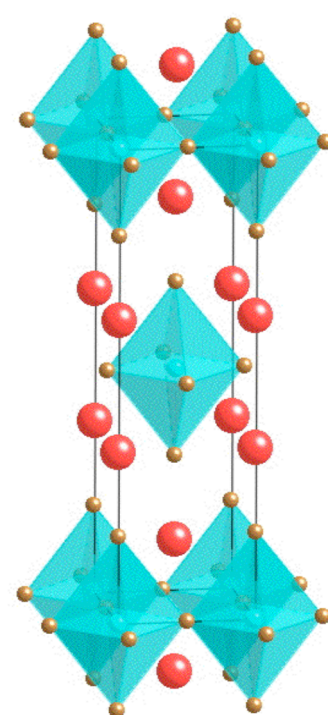
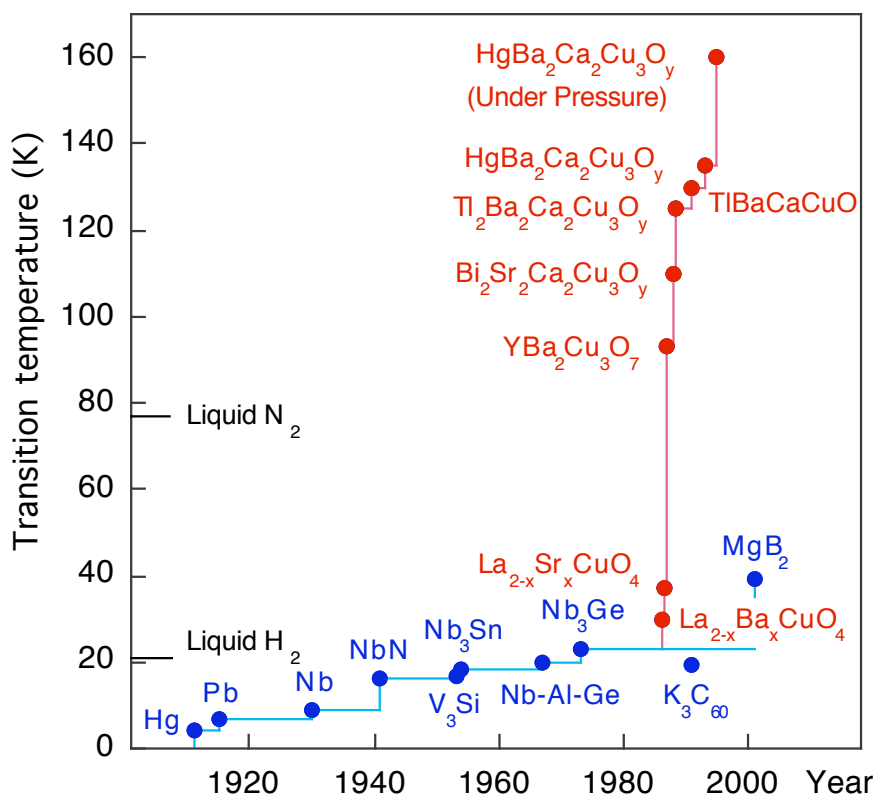
Meissner effect



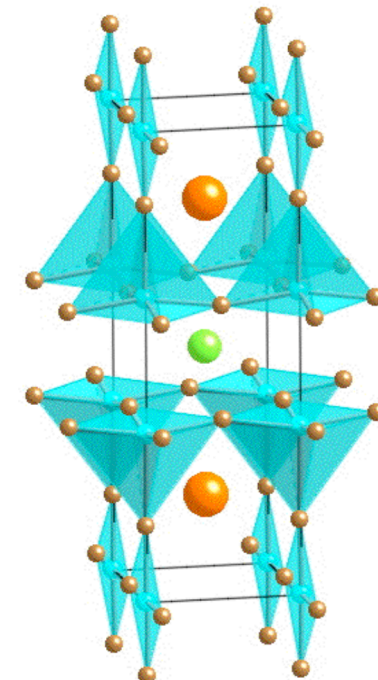
Exclusion of a magnetic field from a superconductor

3. High Temperature Superconductors

Critical Temperature



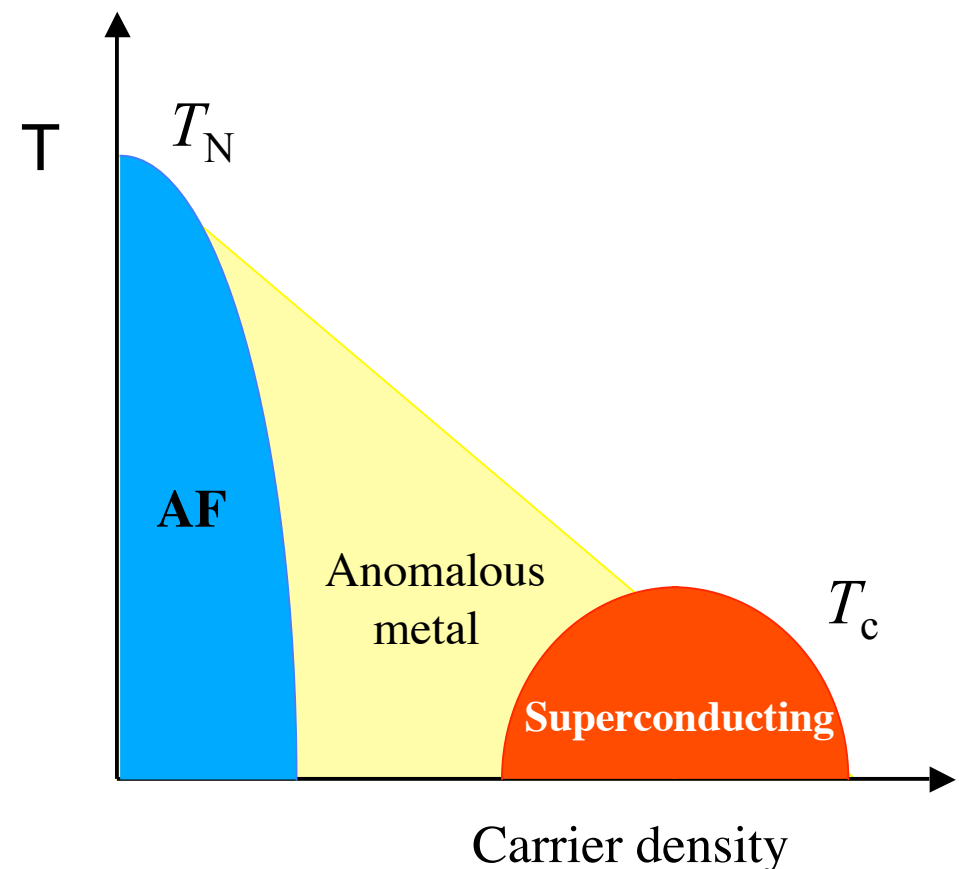
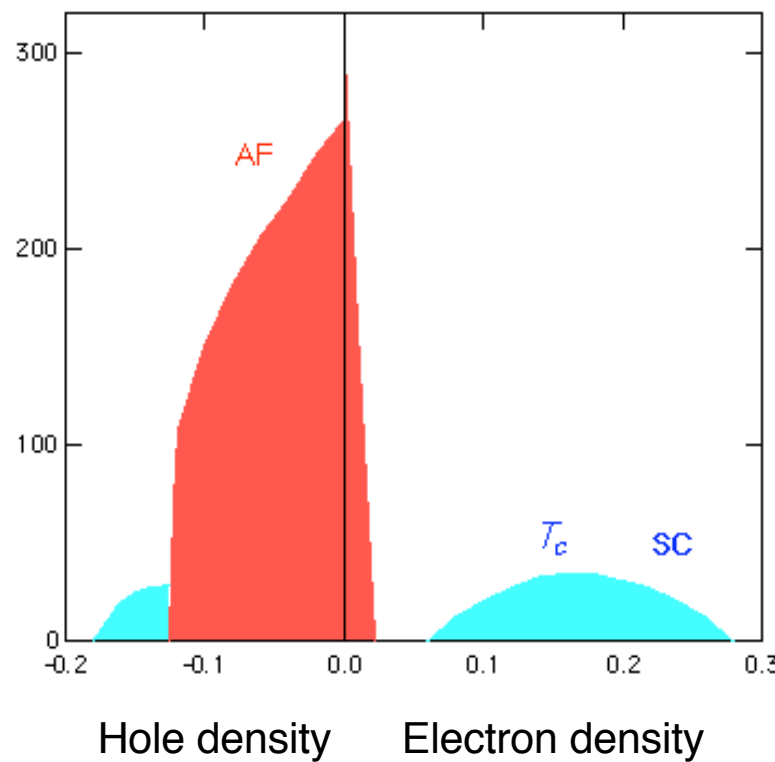
La₂CuO₄



YBa₂Cu₃O₇

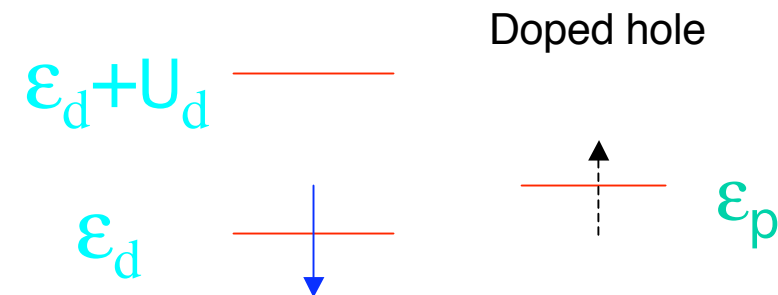
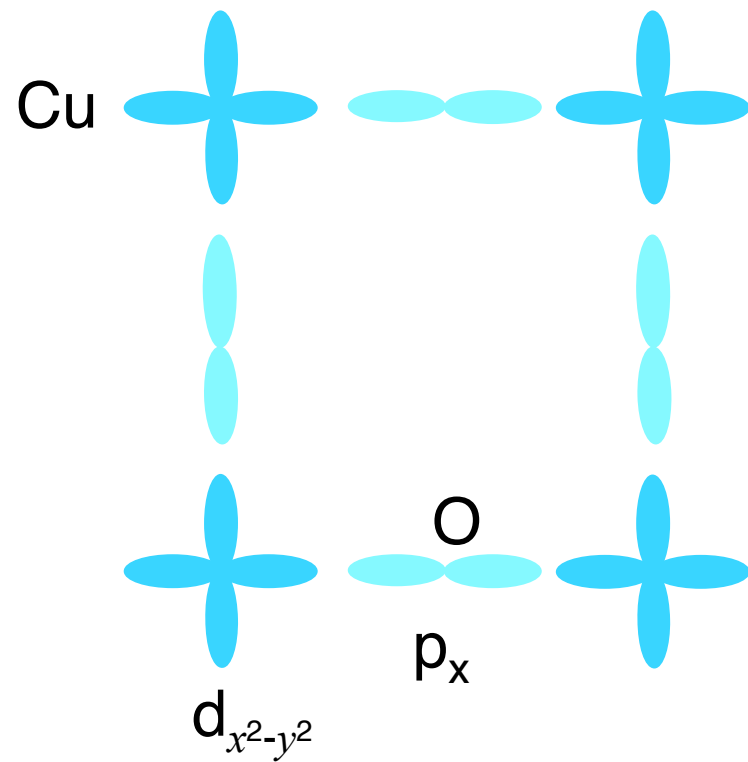
Phase Diagrams

Phase diagram of HTSC



Model of HTSC

Two-Dimensional Plane



Characteristics

- Two dimensional
- Low spin $1/2$
- O level is very closed to Cu level.

Temperature dependence of Resistivity

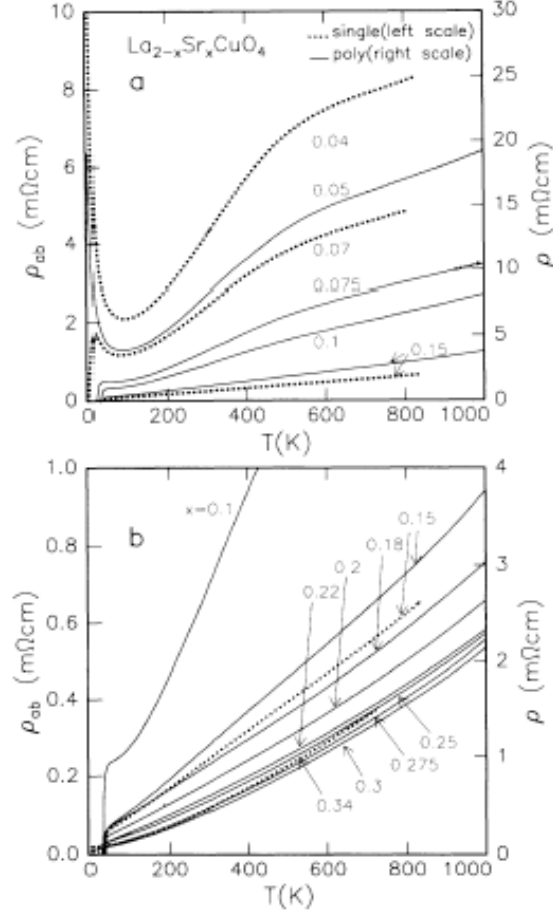


FIG. 1. The temperature dependence of the resistivity for $\text{La}_{2-x}\text{Sr}_x\text{CuO}_4$. (a) $0 < x \leq 0.15$, (b) $0.1 \leq x < 0.35$. Dotted lines, the in-plane resistivity (ρ_{ab}) of single-crystal films with (001) orientation; solid lines, the resistivity (ρ) of polycrystalline materials. Note, $\rho_M = (h/e^2)d = 1.7 \text{ m}\Omega\text{cm}$.

H. Takagi et al.

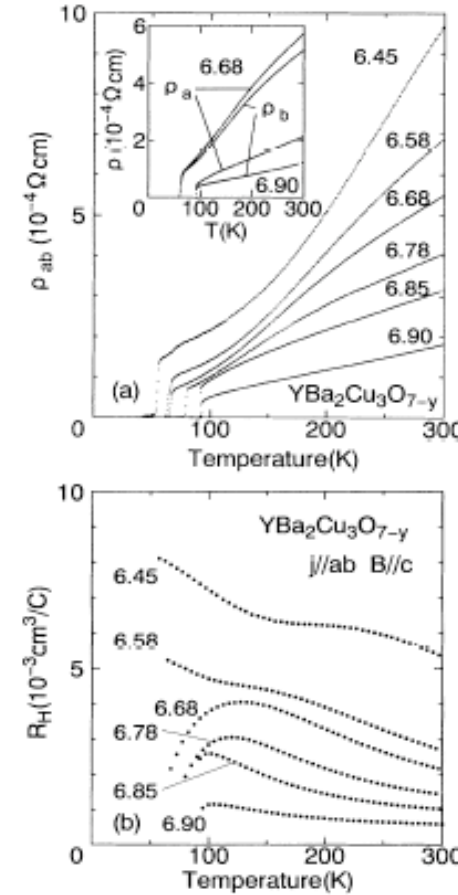


FIG. 1. (a) Temperature dependence of in-plane resistivity of twinned $\text{YBa}_2\text{Cu}_3\text{O}_{7-y}$ crystals with oxygen concentration $7-y \sim 6.90, 6.85, 6.78, 6.68, 6.58$, and 6.45 . Inset: Temperature dependence of ρ_a and ρ_b for detwinned crystals of $T_c=90$ and 60 K. (b) Temperature dependence of R_H of twinned crystals measured under $J \parallel ab$ plane and $\mathbf{B} \parallel c$ axis at $B = 5$ T.

T. Ito et al.

Specific Heat

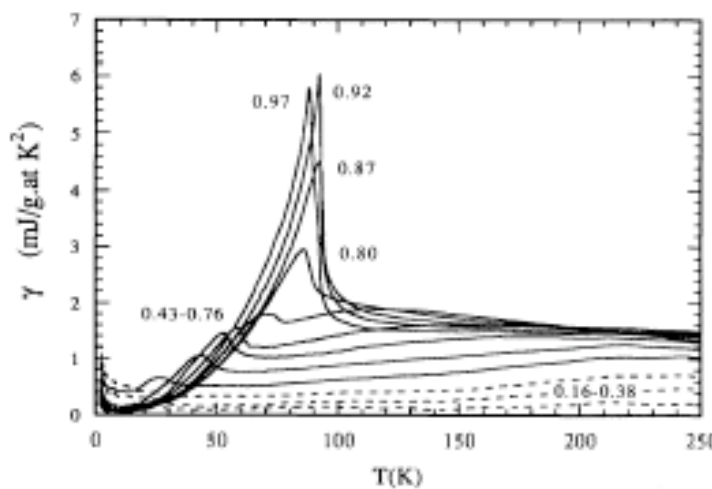


FIG. 4. Electronic specific heat coefficient $\gamma(x,T)$ vs T for $\text{YBa}_2\text{Cu}_3\text{O}_{6+x}$ relative to $\text{YBa}_2\text{Cu}_3\text{O}_6$. Values of x are 0.16, 0.29, 0.38, 0.43, 0.48, 0.57, 0.67, 0.76, 0.80, 0.87, 0.92, and 0.97.

Loram et al., Phys. Rev. Lett. 71, 1740 (1993)

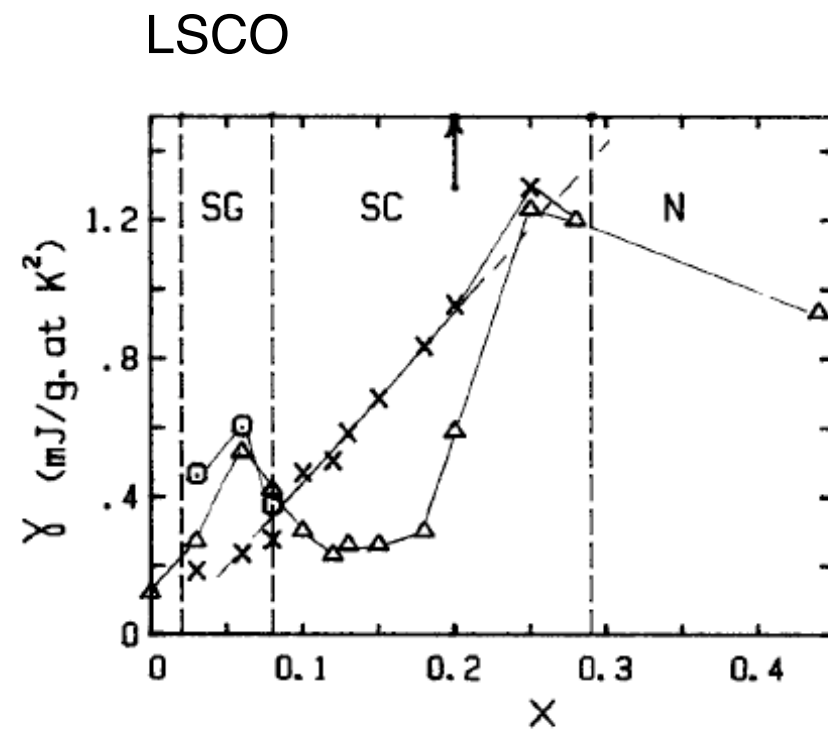


FIGURE 2
 γ vs x . for $x \leq 0.08$ $\Delta, \gamma(2\text{K})$; $\circ, \gamma(8\text{K})$; $\times, \gamma(40\text{K})$
for $x \geq 1$ $\blacktriangle, \gamma(0)$; \times, γ_n

Loram et al., Physica C162-164, 498 (1989)

Nuclear Magnetic Resonance

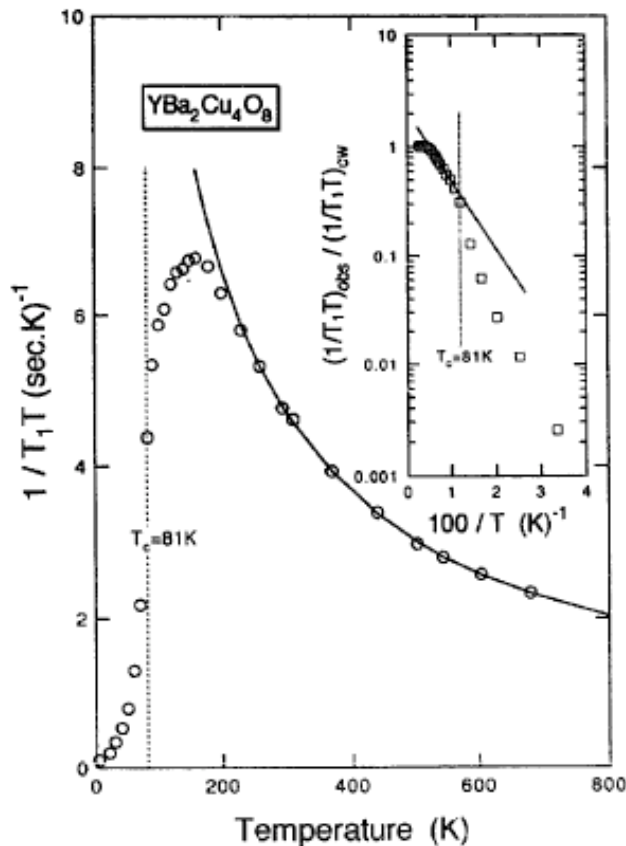


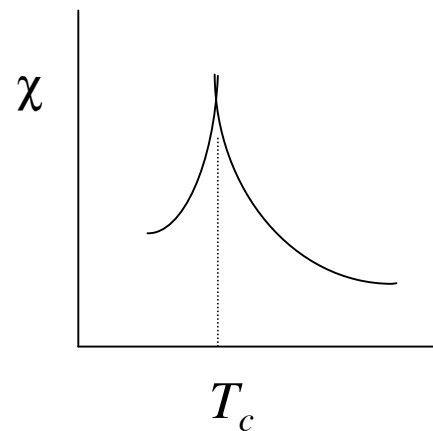
Fig. 1. Temperature dependence of the nuclear spin-lattice relaxation rate $1/T_1T$ for Cu(2) sites of $\text{YBa}_2\text{Cu}_4\text{O}_8$. The solid curve shows the best fit of the data to Eq. (1) for $T > 250$ K. The inset shows the Arrhenius plots for the ratio of the observed $(1/T_1T)_{\text{obs}}$ to the expected $(1/T_1T)_{\text{cw}}$ from Eq. (1), and the best fit of the data to Eq. (2) is shown by the solid line.

$\text{YBa}_2\text{Cu}_4\text{O}_8$

$T_c = 81\text{K}$

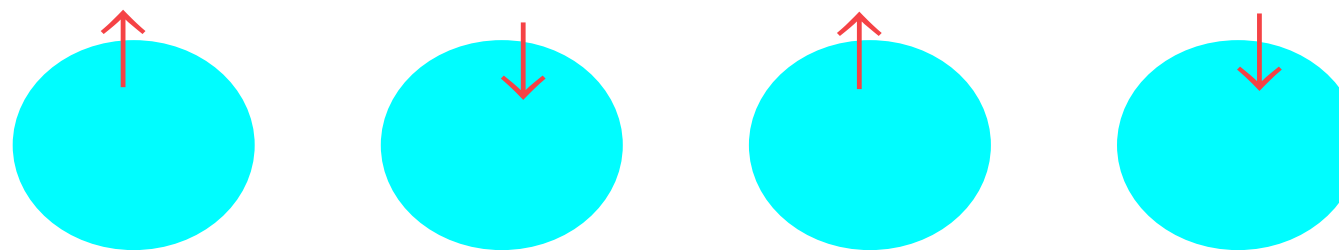
The decrease of $1/T_1T$ above T_c suggests the existence of the pseudo-gap.

In the conventional case



4. Hubbard Model

Itinerant Electrons



Electrons

Atoms

Mott insulators

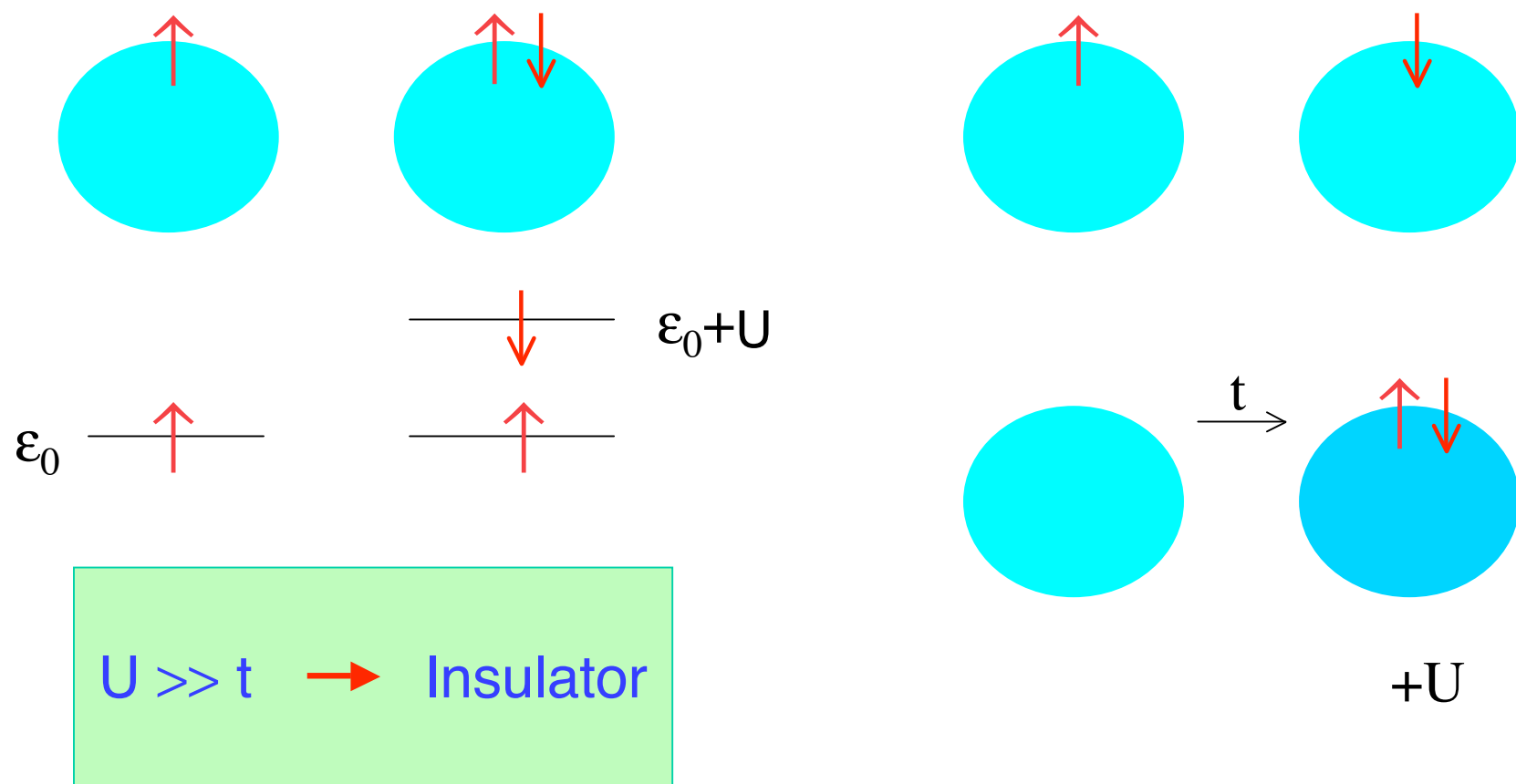
MnO , FeO , CoO , Mn_3O_4 , Fe_3O_4 ,
 NiO , CuO

Insulators due to the Coulomb interaction

(Note: Antiferromagnets such as MnO and NiO are not Mott insulators in the strict sense.)

On-site Coulomb Interaction

Coulomb interaction



Gap in the Hubbard Model

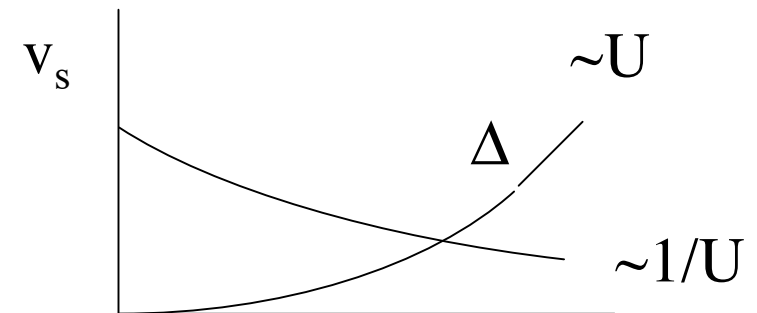
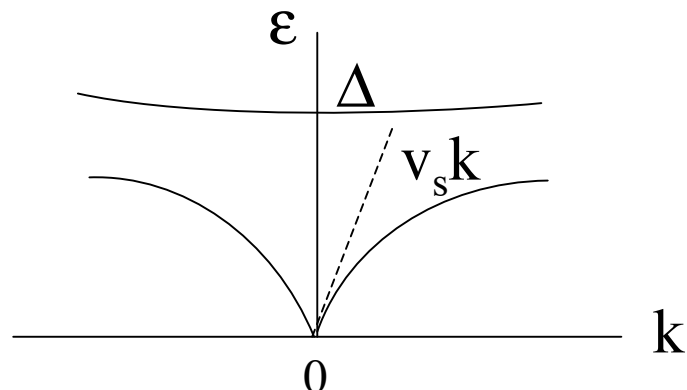
Hartree-Fock theory (Half-filling)

$$\text{AF Gap } \Delta = Um \quad \Delta \sim t e^{-2\pi t/U} \quad d = 1, 3$$

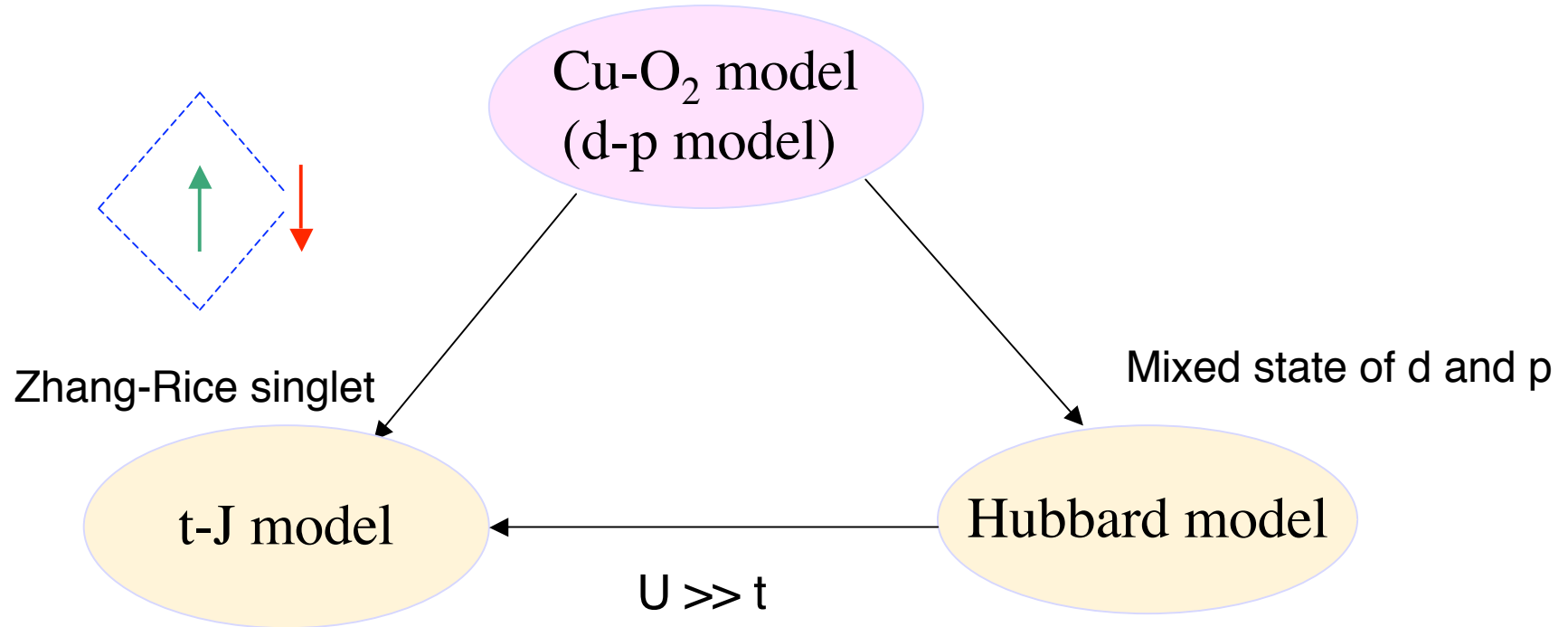
$${} \qquad \qquad \qquad \sim t e^{-2\pi(t/U)^{1/2}} \quad d = 2$$

1D Hubbard model

	$U \ll t$	$U \gg t$
Hubbard gap Δ	$(16/\pi)\sqrt{tU}e^{-\pi/(2U)}$	U
Spin-wave velocity $2v_s/\pi = J$	$(4t/\pi)(1 - U/4\pi t)$	$4t^2/U$



Cu-O₂ Model and Hubbard Model



$$H = -t \sum_{\langle ij \rangle \sigma} (c_{i\sigma}^+ c_{j\sigma} + h.c.) + J \sum_{\langle ij \rangle} S_i \cdot S_j$$

$$H = -t \sum_{\langle ij \rangle \sigma} (c_{i\sigma}^+ c_{j\sigma} + h.c.) + U \sum_i n_{i\uparrow} n_{i\downarrow}$$

$$\begin{aligned} t_{pd} &<< U_d - (\varepsilon_p - \varepsilon_d) \\ t_{pd} &<< \varepsilon_p - \varepsilon_d \\ \varepsilon_p - \varepsilon_d &<< U_d \end{aligned}$$

$$\varepsilon_p - \varepsilon_d \sim 0(t_{pd})$$

5. Variational Monte Carlo method

We evaluate the expectation values using the Monte Carlo method.

Gutzwiller function

$$\Psi_G = P_G \Psi_0$$

Ψ_0 : trial wave function Fermi sea, AF state, or BCS state

$$P_G = \prod_j \left(1 - (1-g)n_{j\uparrow}n_{j\downarrow}\right)$$

Gutzwiller operator

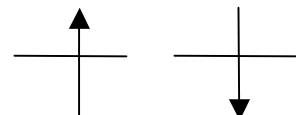
$$0 \leq g \leq 1$$

Control the on-site correlation in terms of g



weight g

Coulomb +U



weight 1

Variational Monte Carlo Method

Normal state

$$\psi_0$$

Slater determinant

$$\psi_0 = \sum_l a_l \psi_l \quad \psi_l : \text{particles in the real space}$$

Wave numbers: k_1, k_2, \dots, k_n

Coordinate positions: j_1, j_2, \dots, j_n

$$\det D_{\uparrow} = \begin{vmatrix} e^{ik_1 j_1} & e^{ik_1 j_2} & \cdots & e^{ik_1 j_n} \\ e^{ik_n j_1} & e^{ik_n j_2} & \cdots & e^{ik_n j_n} \end{vmatrix} \quad \text{Slater determinant}$$

Weight of this state

$$a_l = \det D_{\uparrow} \det D_{\downarrow}$$

The large number of particle configurations → Monte Carlo method

Monte Carlo algorithm

Expectation value

$$\langle \psi Q \psi \rangle = \sum_{mn} a_m a_n \langle \psi_m Q \psi_n \rangle = \sum_m \frac{a_m^2}{\sum_l a_l^2} \sum_n \frac{a_n}{a_m} \langle \psi_m Q \psi_n \rangle$$

The appearance rate of ψ_m is proportional to $P_m = \frac{a_m^2}{\sum_l a_l^2}$ in M.C. steps,

$$\boxed{\langle \psi Q \psi \rangle = \frac{1}{M} \sum_m \left(\sum_n \frac{a_n}{a_m} \langle \psi_m Q \psi_n \rangle \right)} \quad m = 1, \dots, M$$

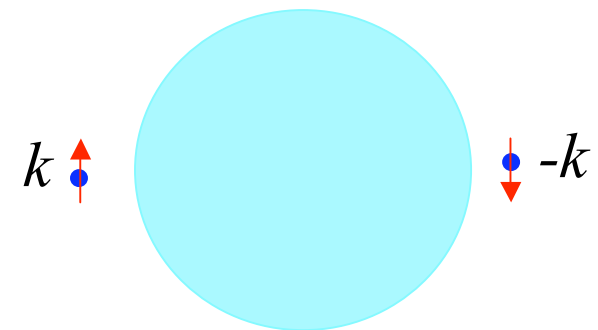
Metropolis法 $\psi_j \rightarrow \psi_n$

If $R = |a_n|^2 / |a_j|^2 \geq \xi$, adopt ψ_n
 $< \xi$ ψ_j again

ξ : random numbers $0 \leq \xi < 1$

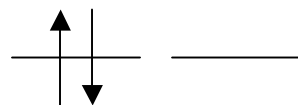
Superconducting state

$$\psi_{CdS} = P_G \prod_k (u_k + v_k c_{k\uparrow}^+ c_{-k\downarrow}^+) |0\rangle$$

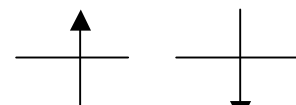


Gutzwiller Projection P_G

To control the on-site strong correlation



Weight g
Coulomb +U



Weight 1
Parameter $0 < g < 1$

Equivalent to
RVB state (Anderson)

Superconducting condensation energy

SC Condensation energy

$$\Delta E_{SC} = \Omega_n - \Omega_s = \int_0^{T_c} (S_n - S_s) dT$$
$$= \int_0^{T_c} (C_s - C_n) dT$$

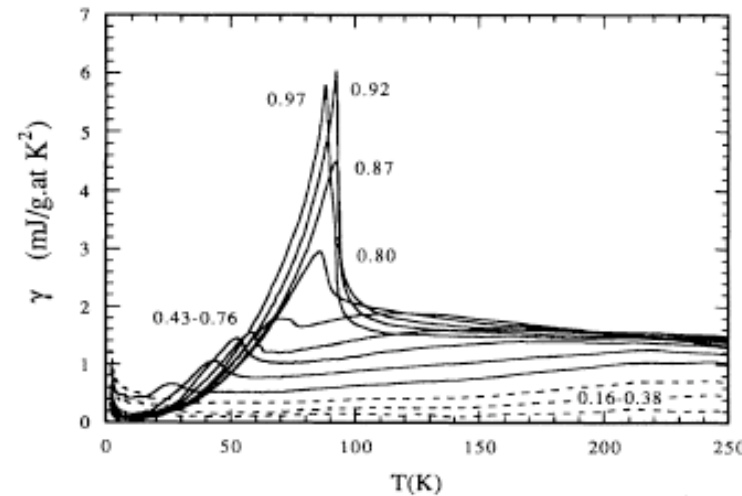
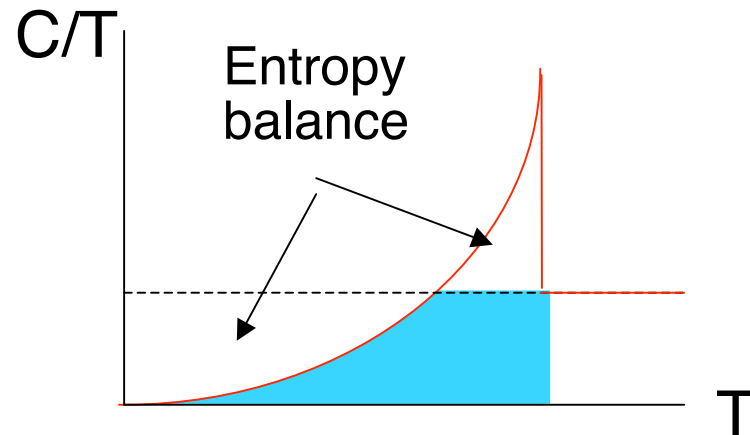
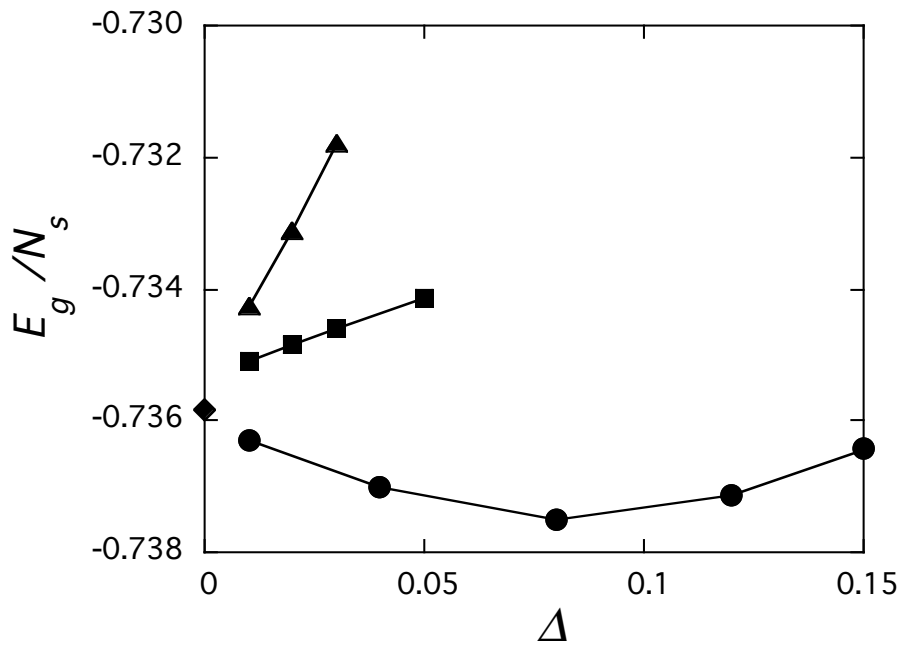


FIG. 4. Electronic specific heat coefficient $\gamma(x, T)$ vs T for $YBa_2Cu_3O_{6+x}$ relative to $YBa_2Cu_3O_6$. Values of x are 0.16, 0.29, 0.38, 0.43, 0.48, 0.57, 0.67, 0.76, 0.80, 0.87, 0.92, and 0.97.

Loram et al. PRL 71, 1740 ('93)
optimally doped YBCO

SC Condensation energy
 ~ 0.2 meV

Evaluations in the superconducting state

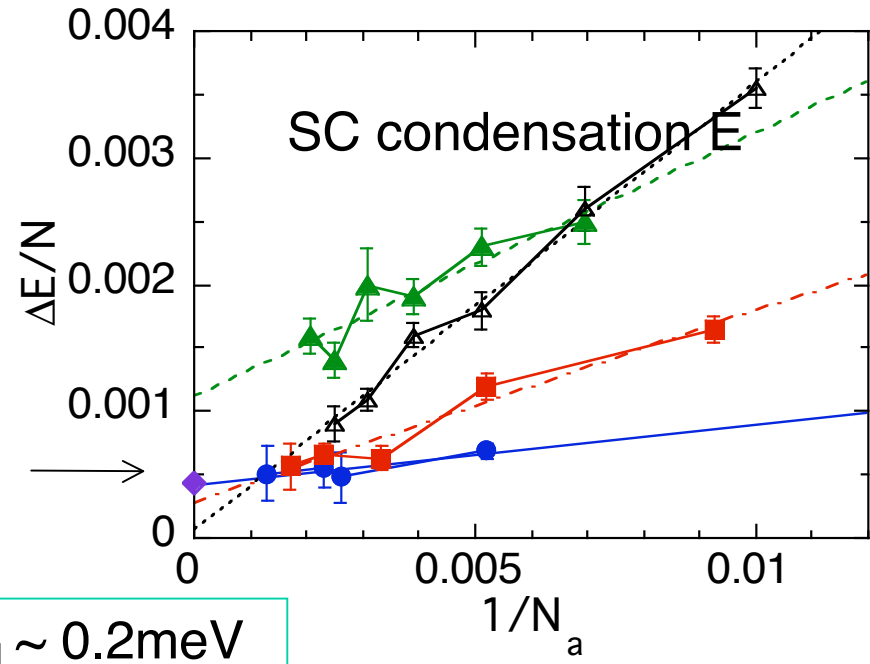


K. Yamaji et al., Physica C304, 225 (1998)
T. Yanagisawa et al.,
Phys. Rev. B67, 132408 (2003)

YBCO

Variational Monte Carlo method
10x10 Hubbard model $U=8$

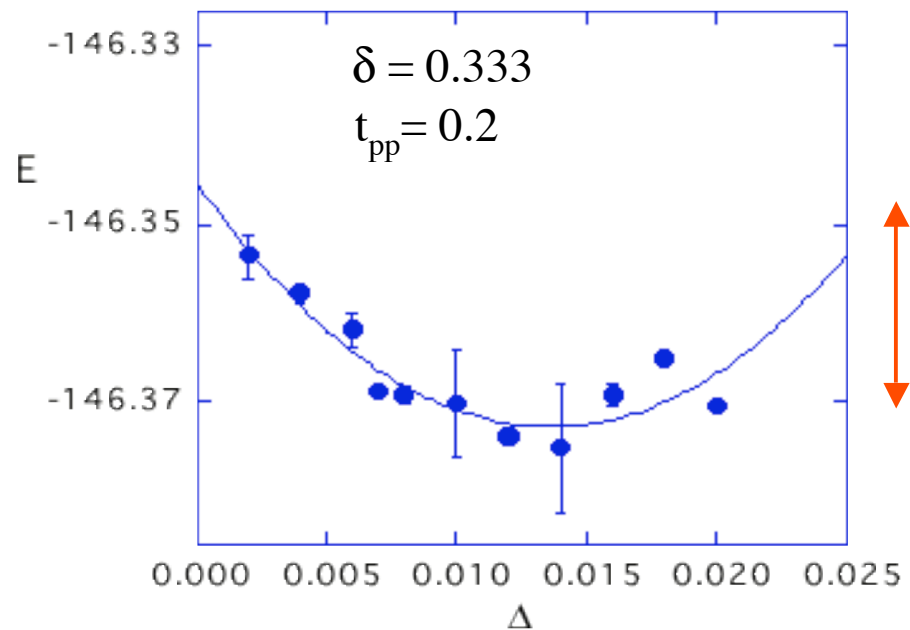
T. Nakanishi et al. JPSJ 66, 294 (1997)



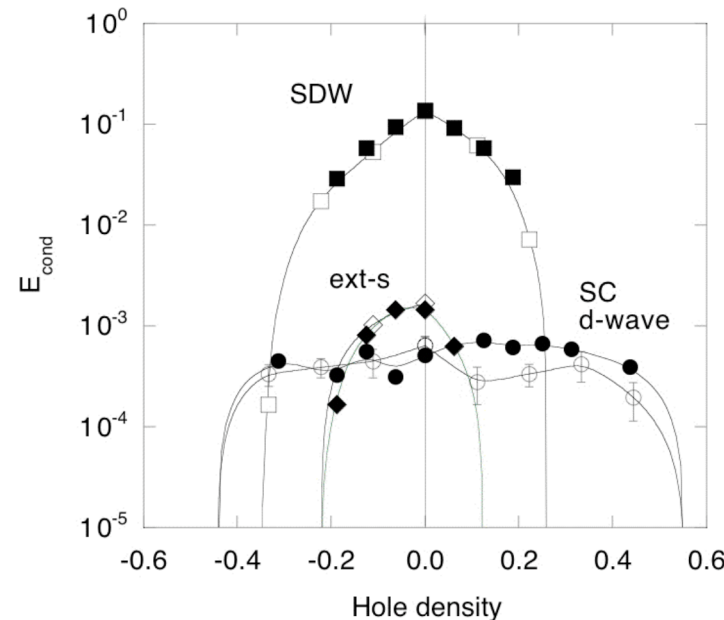
Condensation Energy for d-p model

Condensation energy

$$E_{\text{cond}} \sim 0.00038t_{dp}$$
$$= 0.56 \text{ meV/site}$$



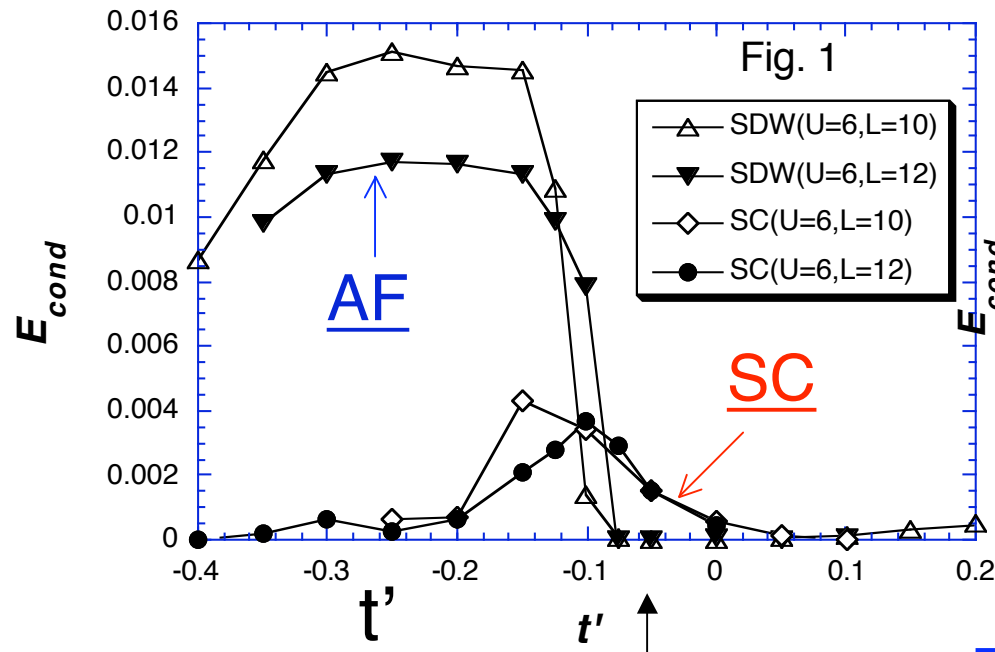
2D d-p model
6x6 and 8x8



T.Yanagisawa et al., PRB64, 184509 ('01)

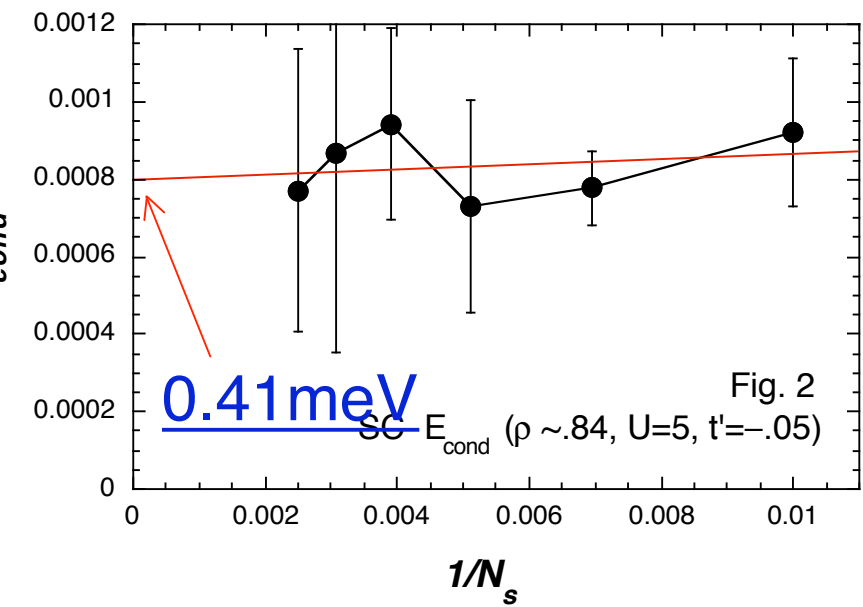
Superconductivity and Antiferromagnetism

Competition



Pure d-wave SC

Size dependence of
SC condensation energy

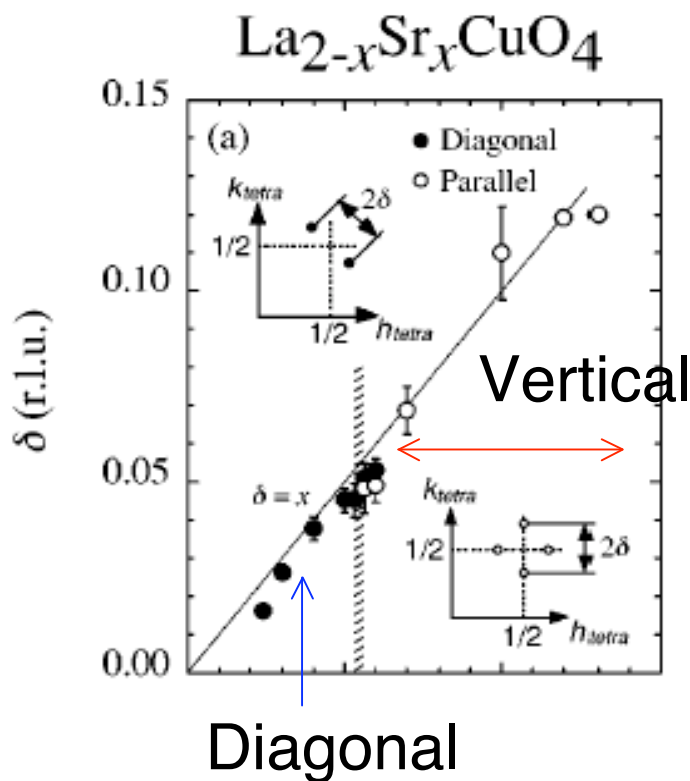


Experiments

0.26 meV/site 0.17~0.26
(critical field H_c) (C/T)

6. Stripes in high-T_c cuprates

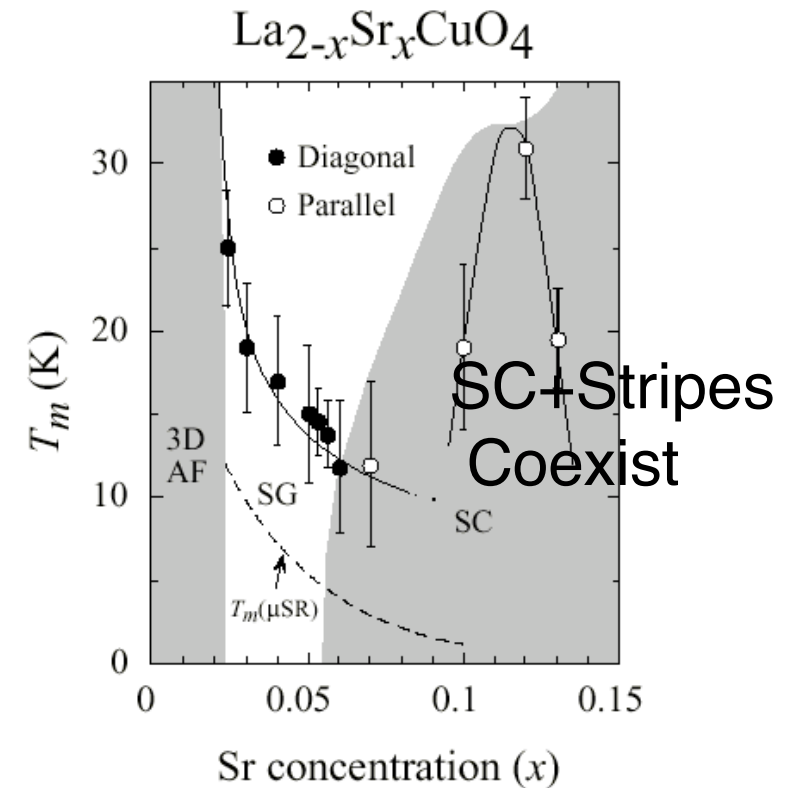
- Vertical stripes for $x > 0.05$
- Diagonal stripes for $x < 0.05$



M.Fujita et al. Phys. Rev.B65,064505('02)

AF coexists with SC?

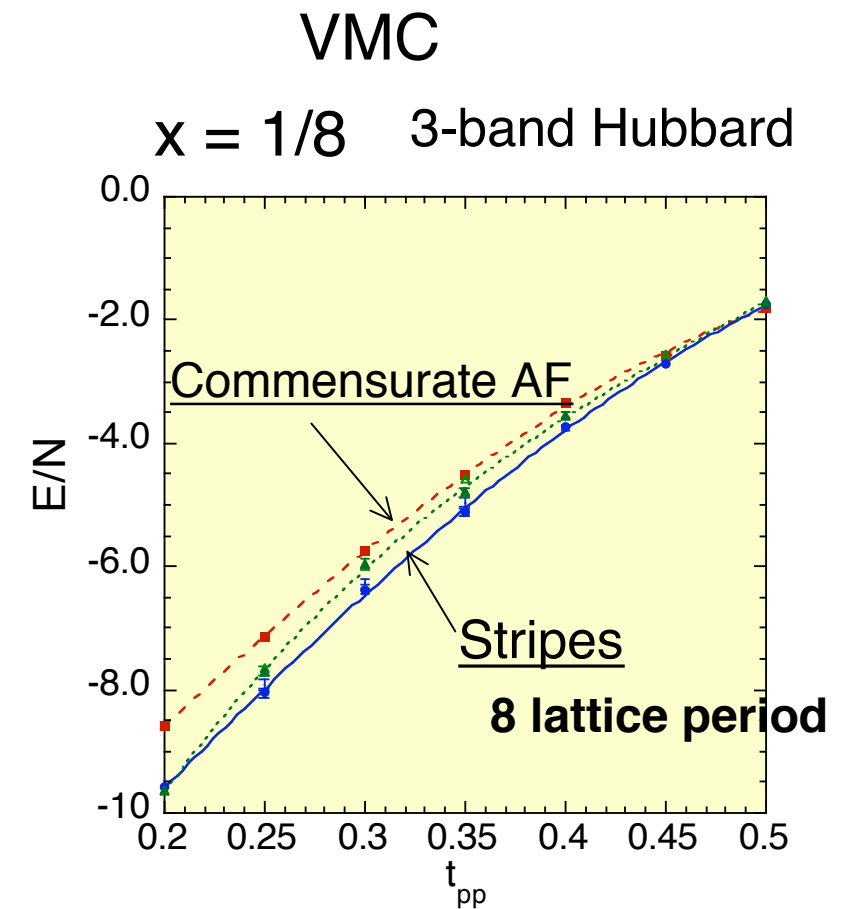
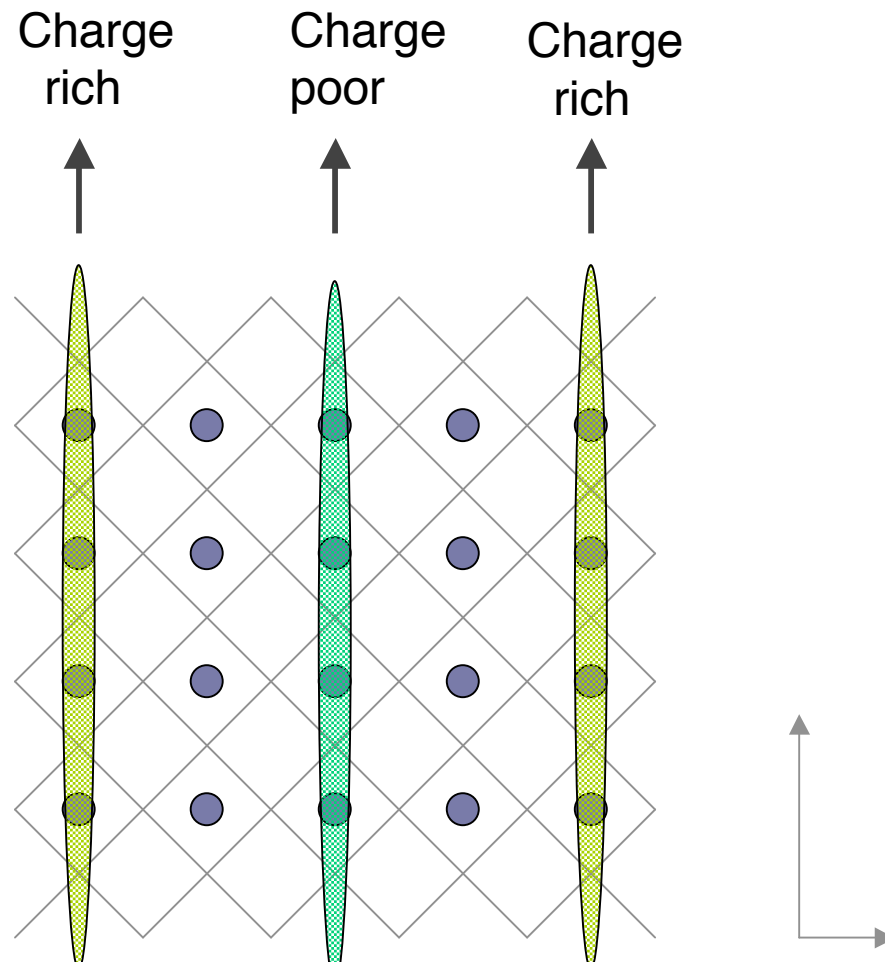
Neutron scattering



S.Wakimoto et al. PRB61, 3699('00)

Vertical Stripes in the under-doped region

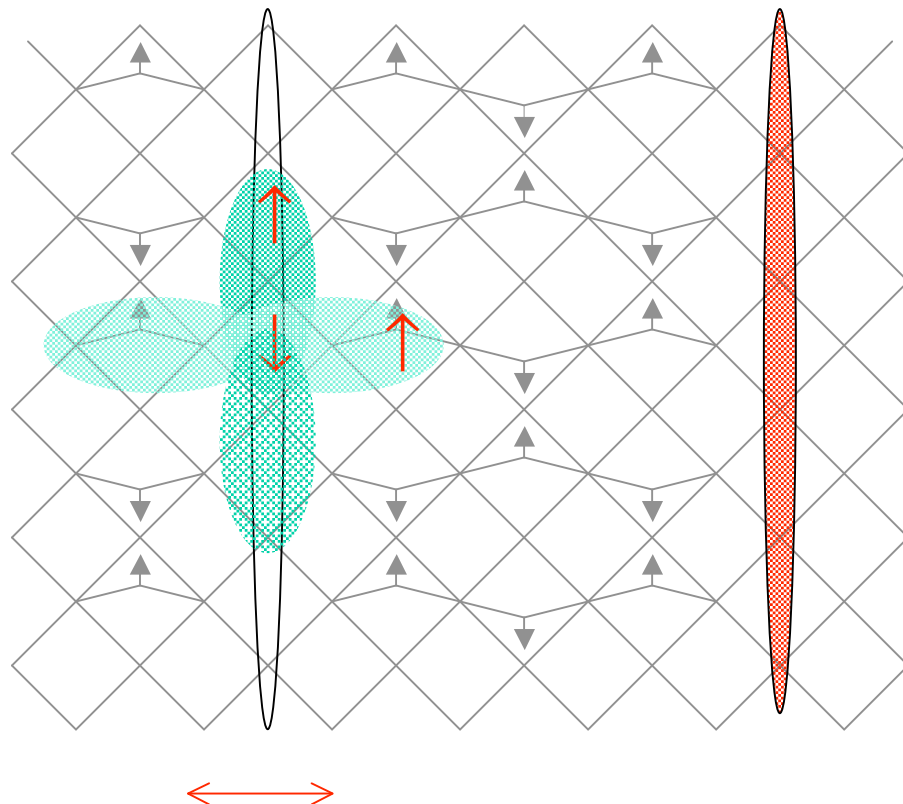
Vertical stripes: 8 lattice periodicity (Tranquada)



T.Y. et al., J.Phys.C14,21('02)

Stripes and Superconductivity

Compete and Collaborate



SC coexists with stripes (AF)

Bogoliubov-de Gennes eq.

$$\begin{pmatrix} H_{ij\uparrow} + F_{ij} \\ F_{ji}^* - H_{ji\downarrow} \end{pmatrix} \begin{pmatrix} u_j^\lambda \\ v_j^\lambda \end{pmatrix} = E^\lambda \begin{pmatrix} u_i^\lambda \\ v_i^\lambda \end{pmatrix}$$

$$\alpha_\lambda = u_i^\lambda a_{i\uparrow} + v_i^\lambda a_{i\downarrow}^+$$

$$\bar{\alpha}_\lambda = \bar{u}_i^\lambda a_{i\uparrow} + \bar{v}_i^\lambda a_{i\downarrow}^+$$

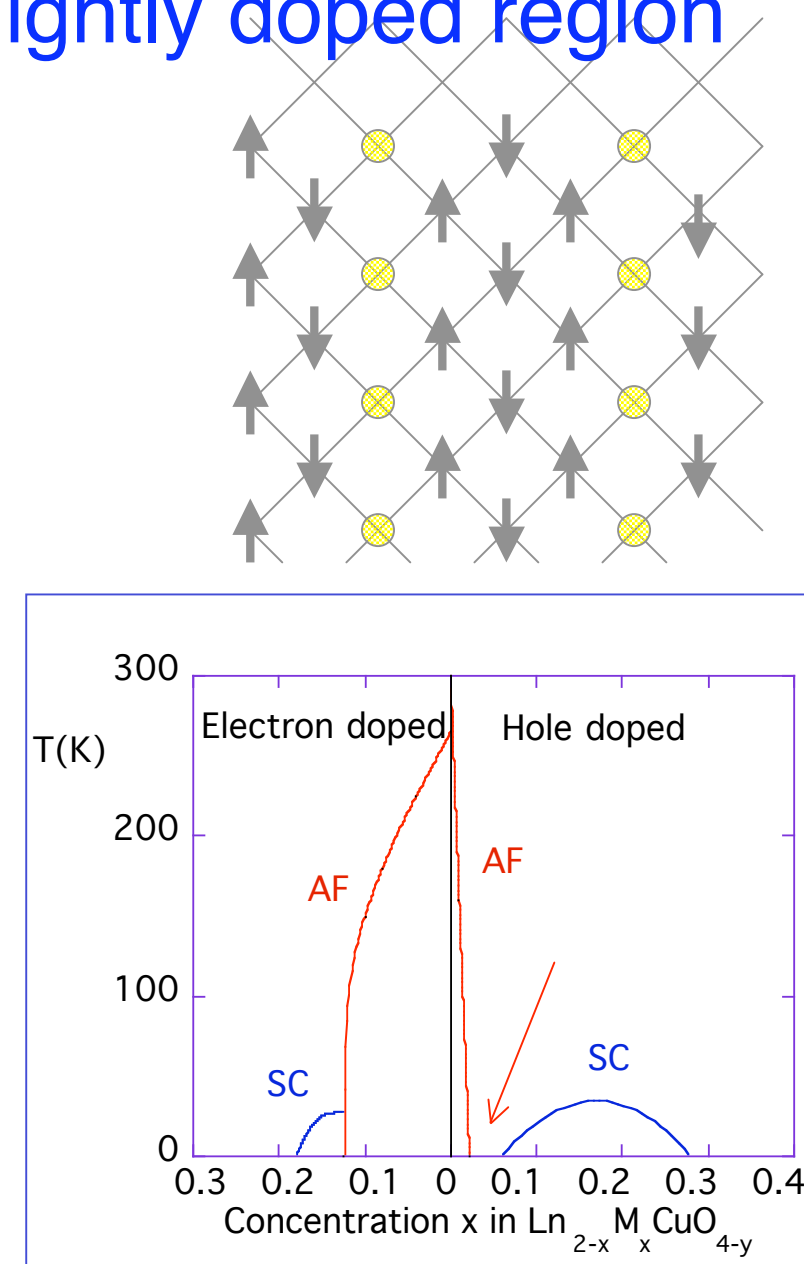
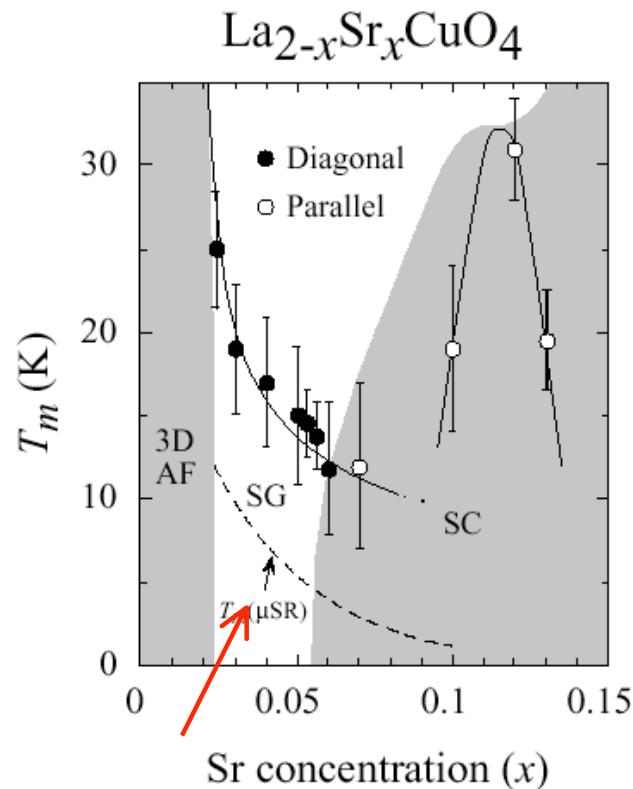
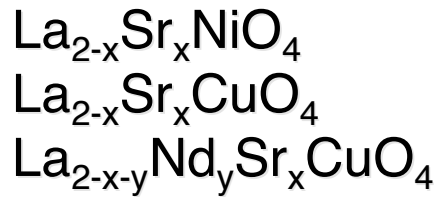
Wave function

$$V_{\lambda j} = v_j^\lambda \quad (\bar{U})_{\lambda j} = \bar{u}_j^\lambda$$

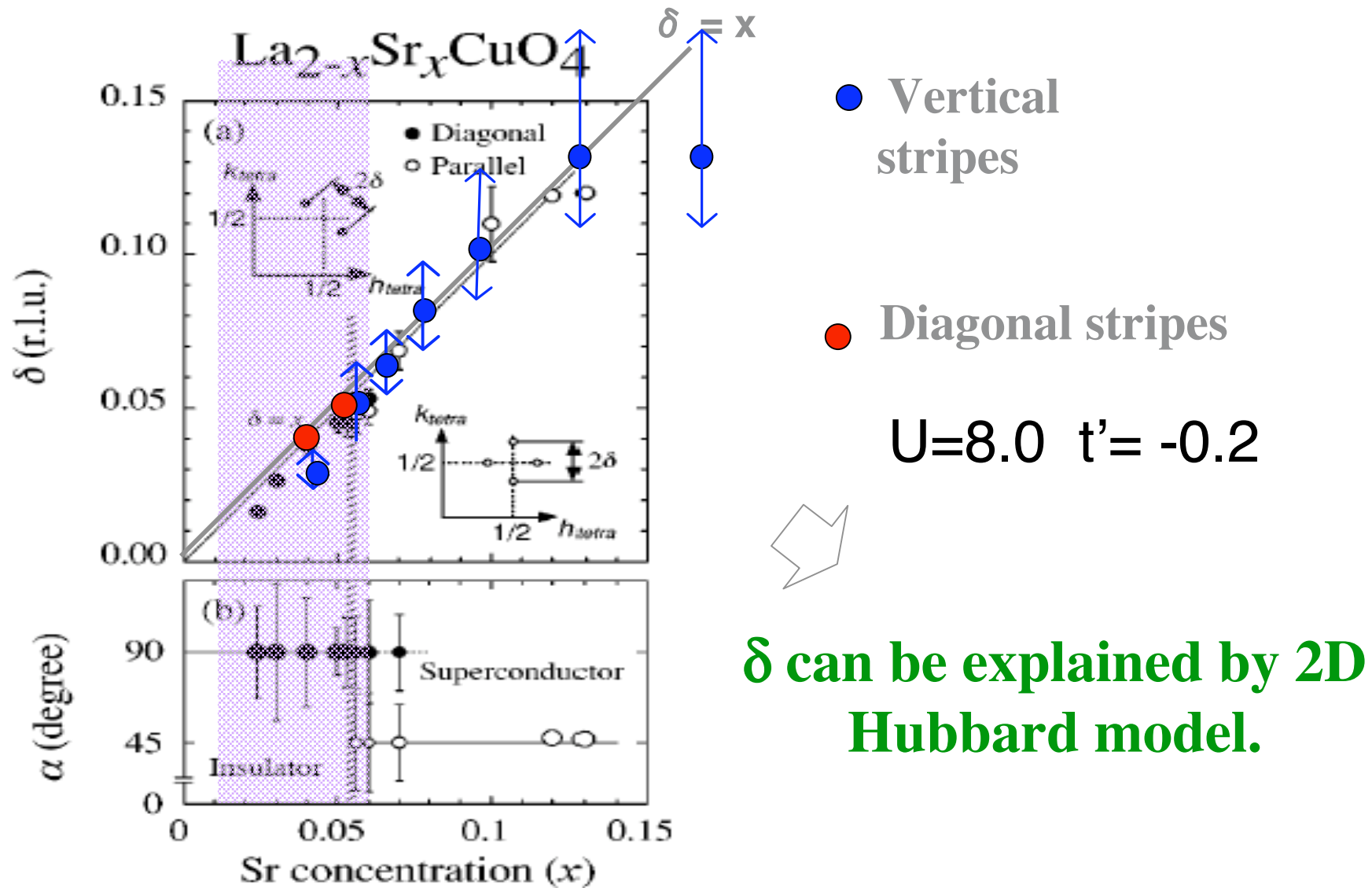
$$\psi_{SC} = P_G P_{N_e} \prod_\lambda \alpha_\lambda \bar{\alpha}_\lambda^+ |0\rangle \propto P_G \left(\sum_{ij} (U^{-1} V)_{ij} a_{i\uparrow}^+ a_{j\downarrow}^+ \right)^{N_e/2} |0\rangle$$

Diagonal stripes in lightly doped region

Diagonal stripes are observed for



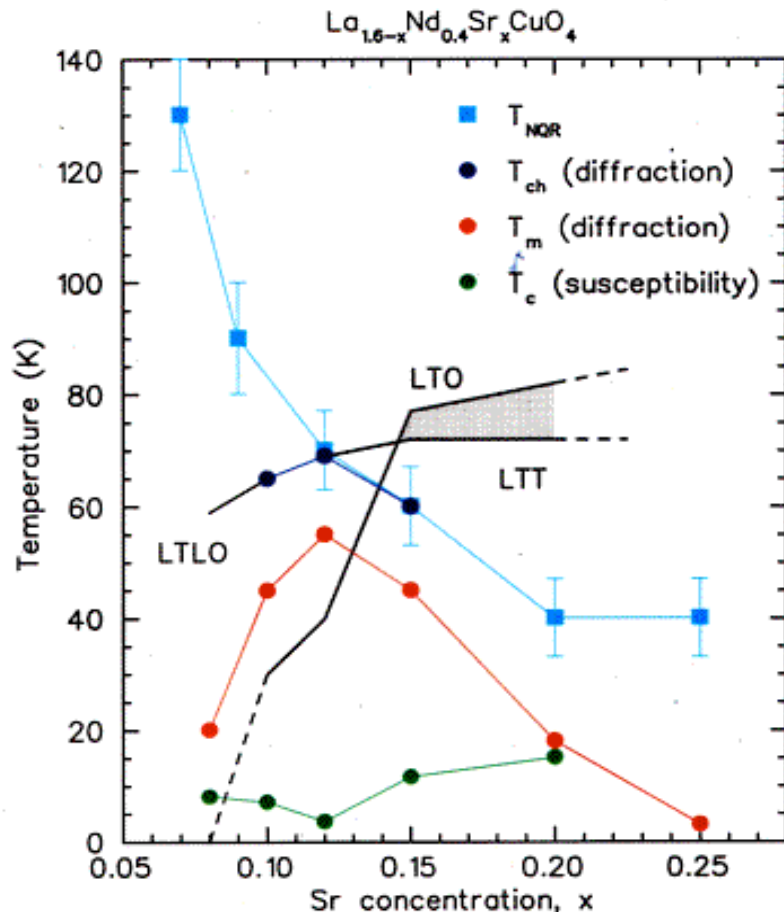
Incommensurability: Comparison with Experiments



Stripes and Structural transition

Structural transitions: Lattice distortions
LTT,LTO,LTLO,HTT

Stripes: suggested by Incommensurability



N.Ichikawa et al.
PRL85, 1738('00)

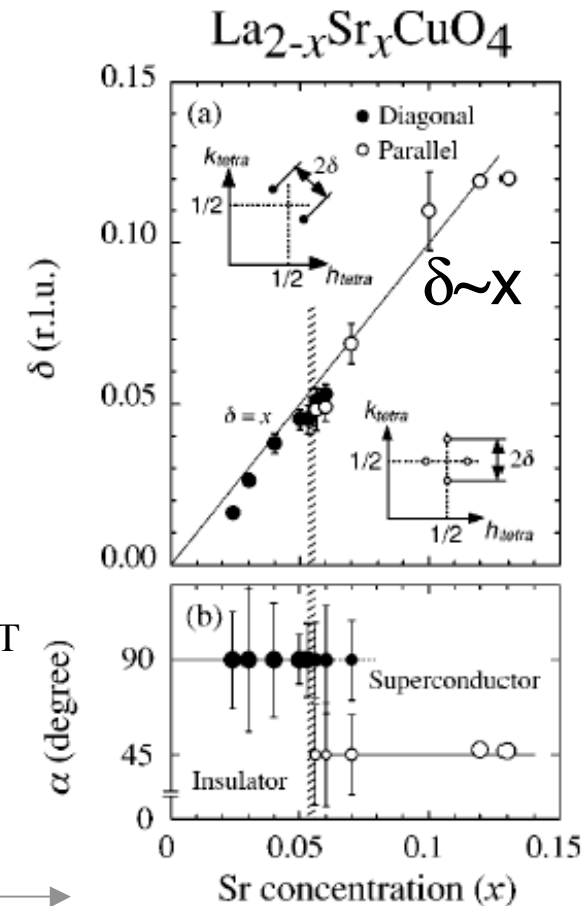
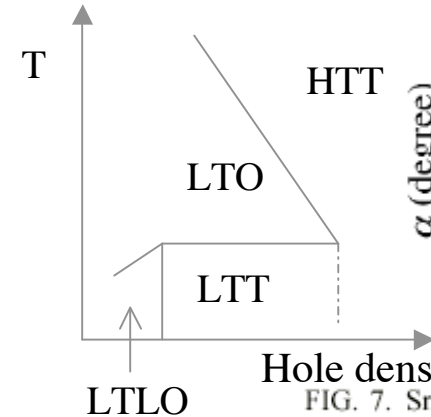


FIG. 7. Sr-concentration dependence of (a) the incommensurability δ and (b) the angle α defined in Fig. 3. Previous results for $x=0.024$ (Ref. 11), 0.04 (Ref. 10), 0.05 (Ref. 10), 0.12 (Ref. 5), 0.1 (Ref. 15), and 0.13 (Ref. 15) are included. In both figures, the solid and open symbols represent the results for the diagonal and parallel components, respectively.

M.Fujita et al. Phys. Rev.B65,064505('02)

What happens under lattice distortions

1. Anisotropy of the transfer integrals

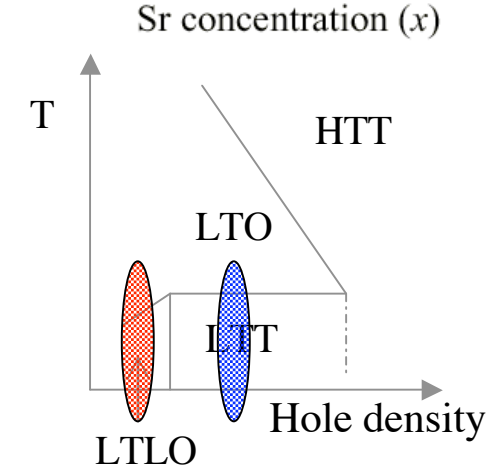
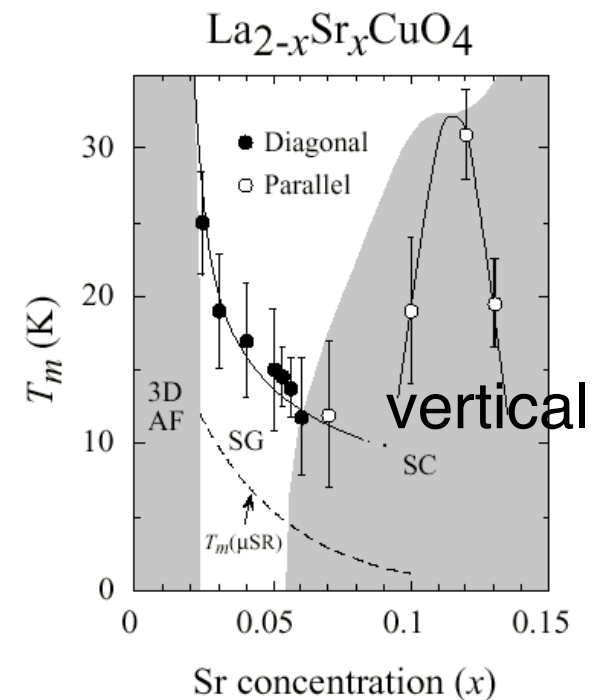
Anisotropic electronic state

vertical stripes

Diagonal stripes $x < 0.05$

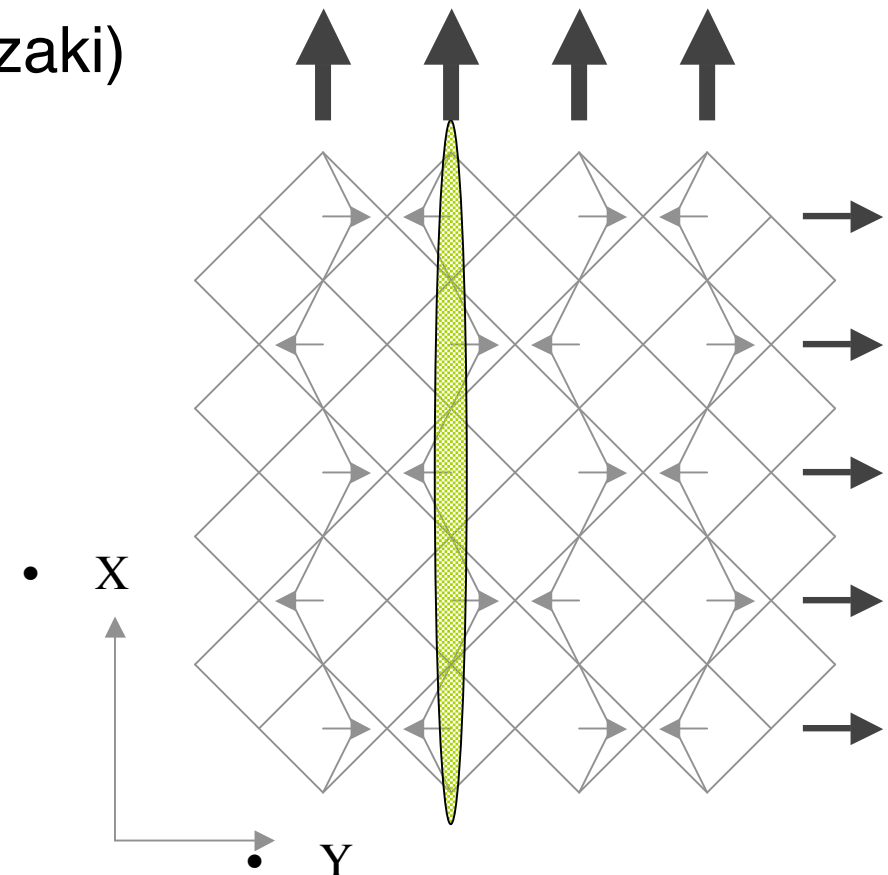
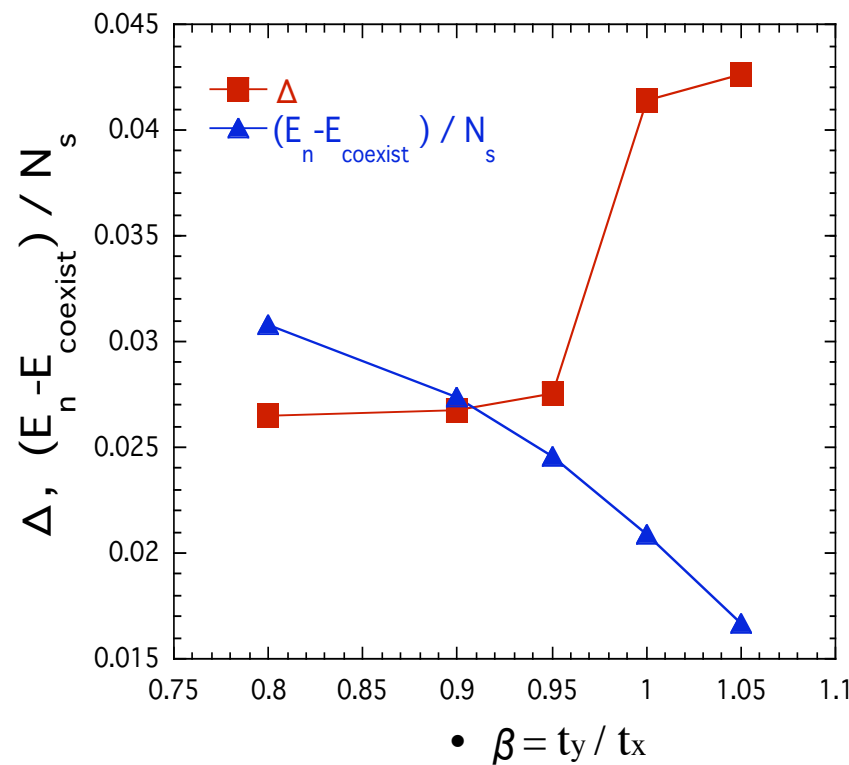
2. Spin-Orbit Coupling induced from lattice distortions

3. Electron-phonon interaction



Anisotropy of the transfer integrals in LTT phase

One-band Hubbard model (Miyazaki)



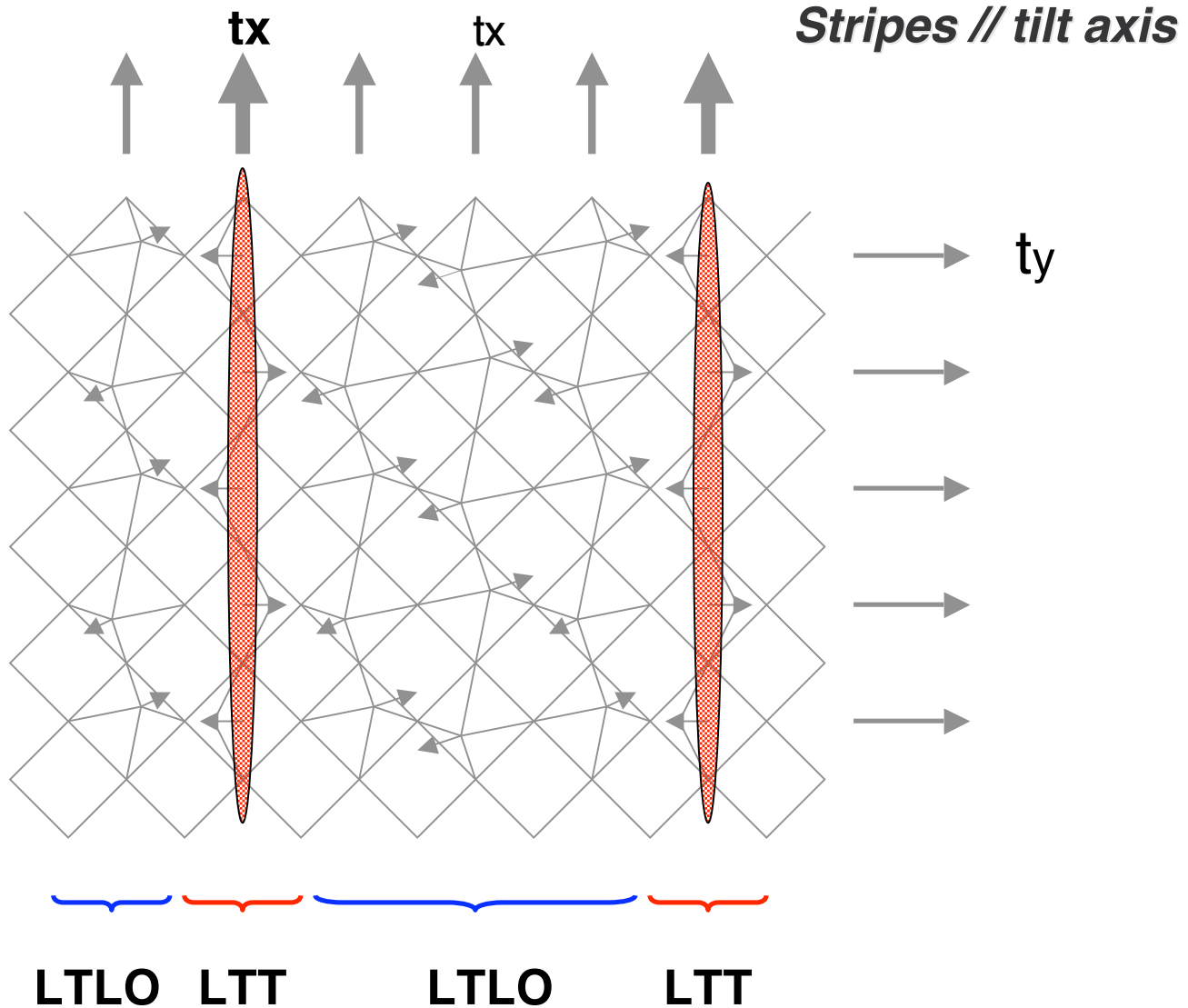
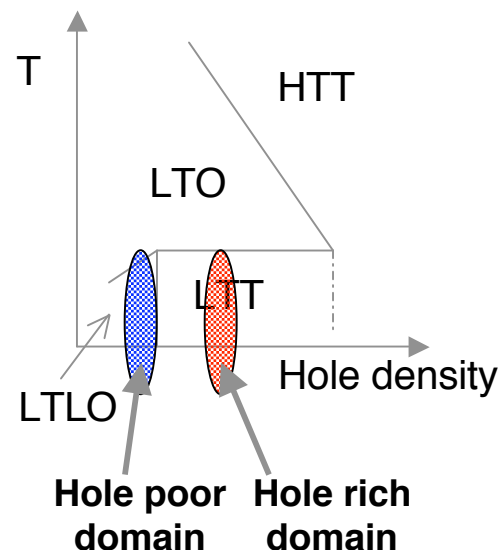
LTT structural transitions stabilize stripes.

Possible Stripe Structure 1

Mixed phase of LTT and LTLO

Stabilize stripes

M. K. Crawford et. al.



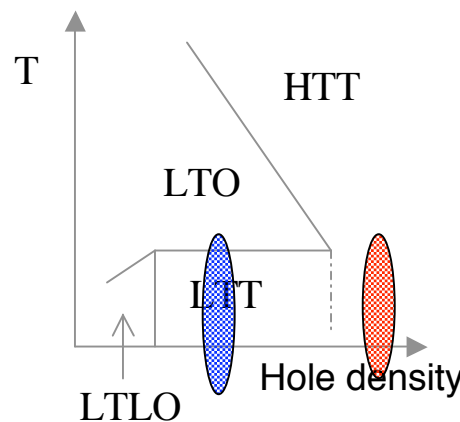
Possible Stripe Structure

Mixed phase of LTT and HTT

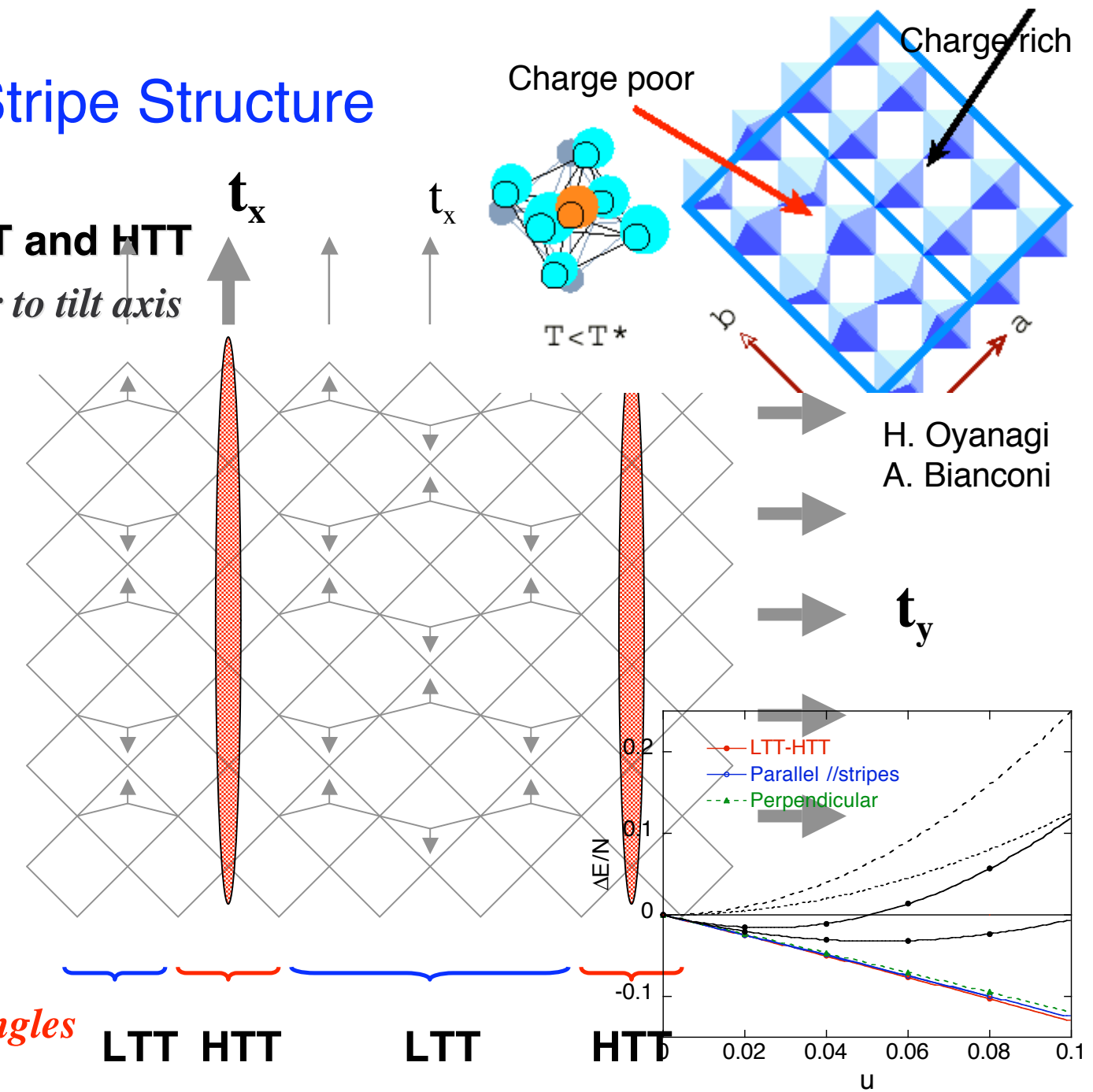
Stripes perpendicular to tilt axis

Stable

M. K. Crawford et. al.



Oscillation of tilt angles



7. Spin-orbit coupling and Lattice distortion

Spin-Orbit Coupling induced by the Lattice distortion

Tilting

Friedel et al., J.Phys.Chem.Solids 25, 781 (1964)

$$\langle p_x(x - a/2, y)^\uparrow | H_{dp} | d_{xz}(r)^\uparrow \rangle = -t_{xz} e^{-ik_x/2 \cdot a}$$

$$\langle p_y(x, y - a/2)^\uparrow | H_{dp} | d_{yz}(r)^\uparrow \rangle = -t_{yz} e^{-iky/2 \cdot a}$$

$$H_{SO} = \xi(r) \mathbf{L} \cdot \mathbf{S}$$

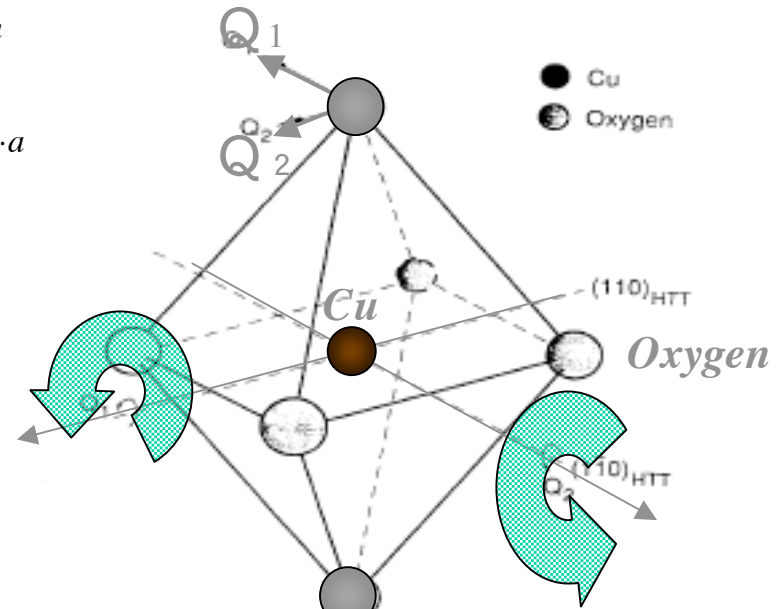
$$\langle d_{xz}(r)^\uparrow | H_{SO} | d_{yz}(r)^\uparrow \rangle = -\frac{i}{2} \xi$$

$$\langle d_{yz}(r)^\uparrow | H_{SO} | d_{xz}(r)^\uparrow \rangle = \frac{i}{2} \xi$$

$$\langle d_{x^2-y^2}(r)^\uparrow | H_{SO} | d_{yz}(r)^\downarrow \rangle = \frac{i}{2} \xi$$

$$\langle d_{x^2-y^2}(r)^\uparrow | H_{SO} | d_{xz}(r)^\downarrow \rangle = \frac{1}{2} \xi$$

Effective $i\xi$ term for p-p transfer



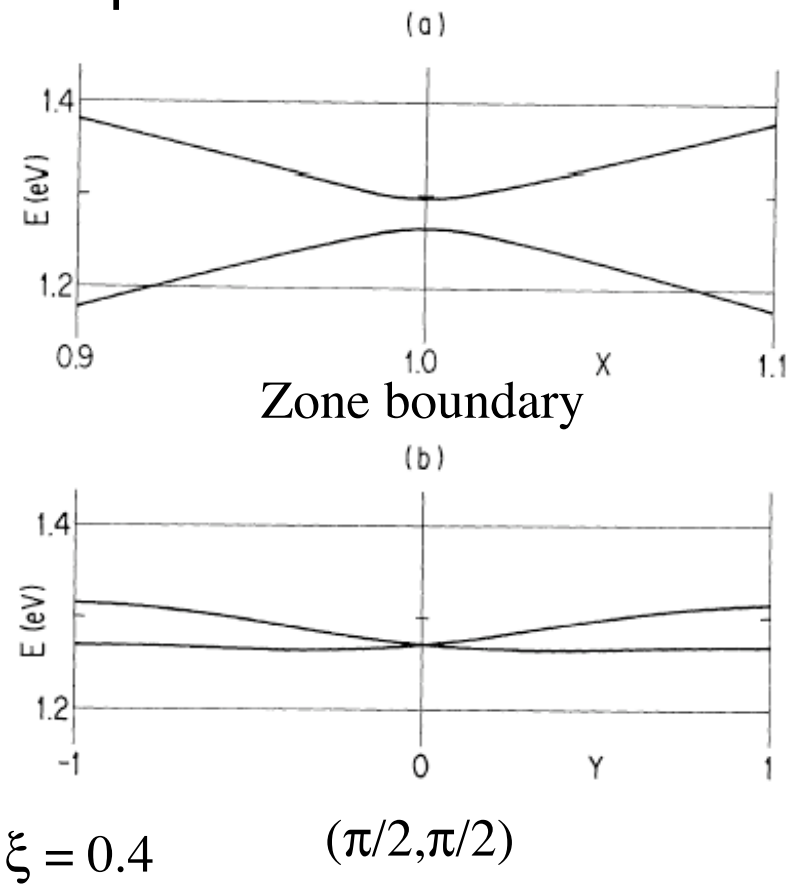
$t_{xz}, t_{yz} \neq 0 \sim \text{tilt angle}$

Five orbitals $\times (\uparrow\downarrow)$:

$(d_{x^2-y^2}, d_{xz}, d_{yz}, p_x, p_y)$

Dispersion in the presence of spin-orbit coupling

d-p model

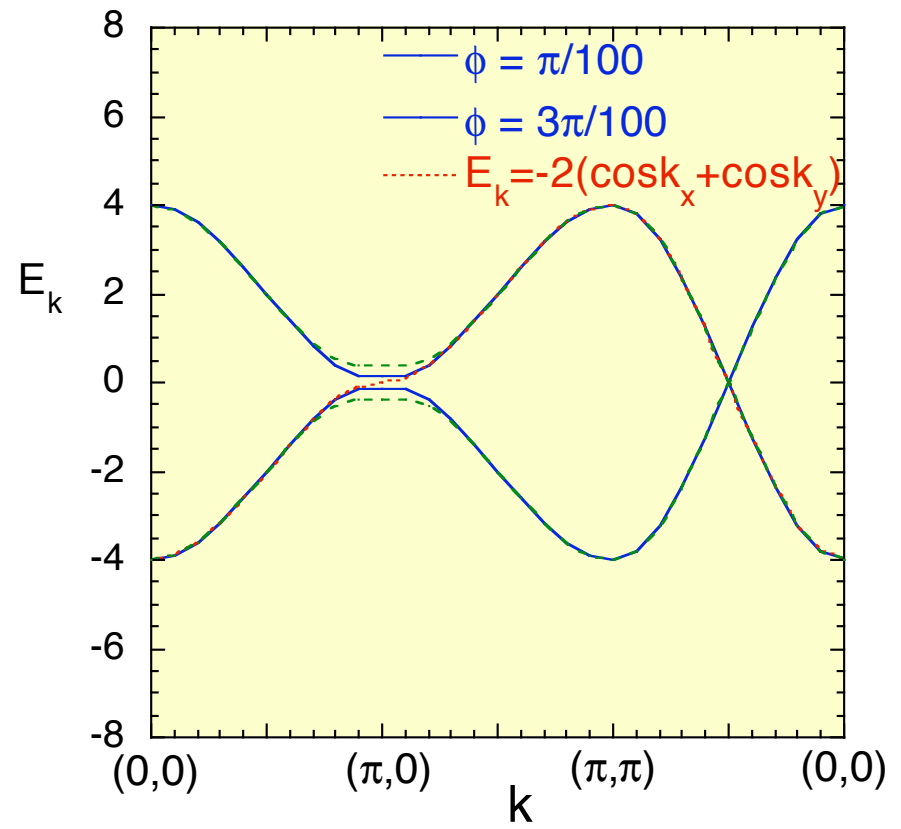


K.Yamaji, JPSJ 57 (1988) 2745.
T.Y. et al., JPSJ 74 (2005) 835.

One-band effective model

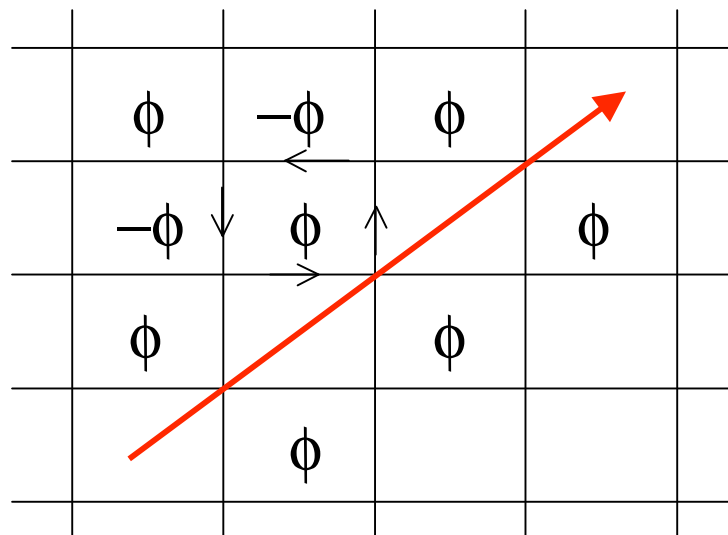
$$H_{kin} = - \sum_{ij\sigma} (t_{ij} + i c \sigma \theta_{ij}) d_{i\sigma}^+ d_{j\sigma}$$

(Bonesteal et al., PRL68,2684('92))



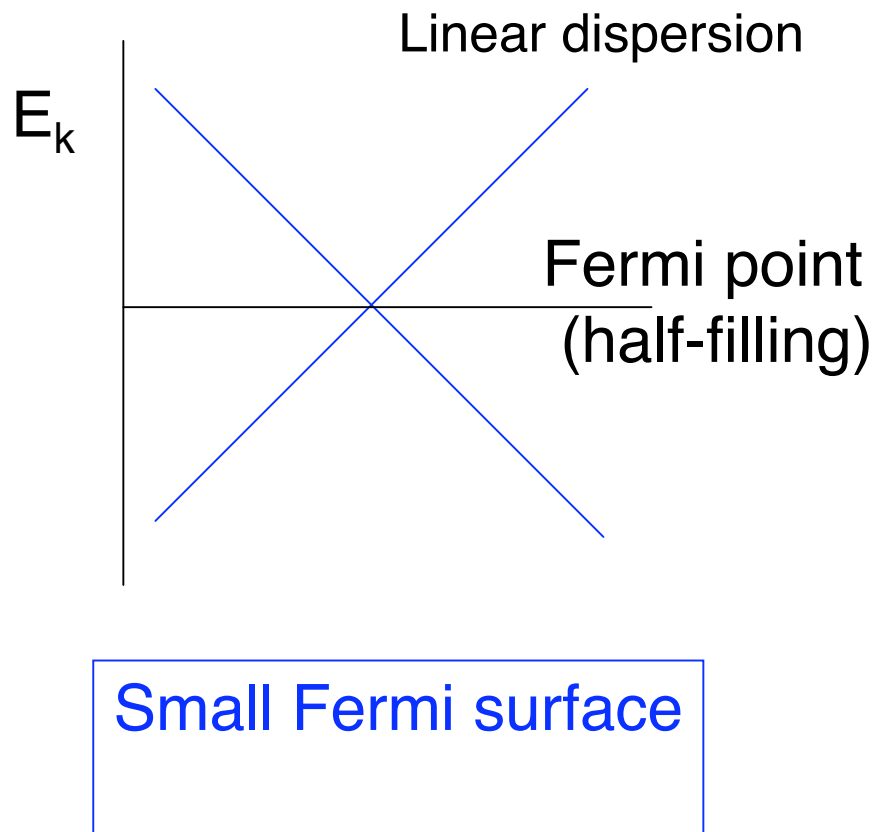
Flux state

$$E(k_x, k_y) = \pm \left| e^{i\phi/4} e^{ik_x} + e^{-i\phi/4} e^{ik_y} + e^{i\phi/4} e^{-ik_x} + e^{-i\phi/4} e^{-ik_y} \right|$$



Inhomogeneous d-density wave

Excitation: Dirac fermion



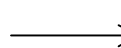
Linear dispersion

Fermi point
(half-filling)

Small Fermi surface

Pseudo-gap in the density of states

Flux state



Pseudo-gap

An origin of pseudo-gap

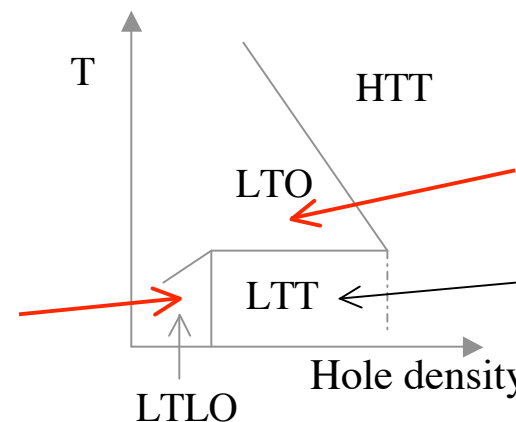
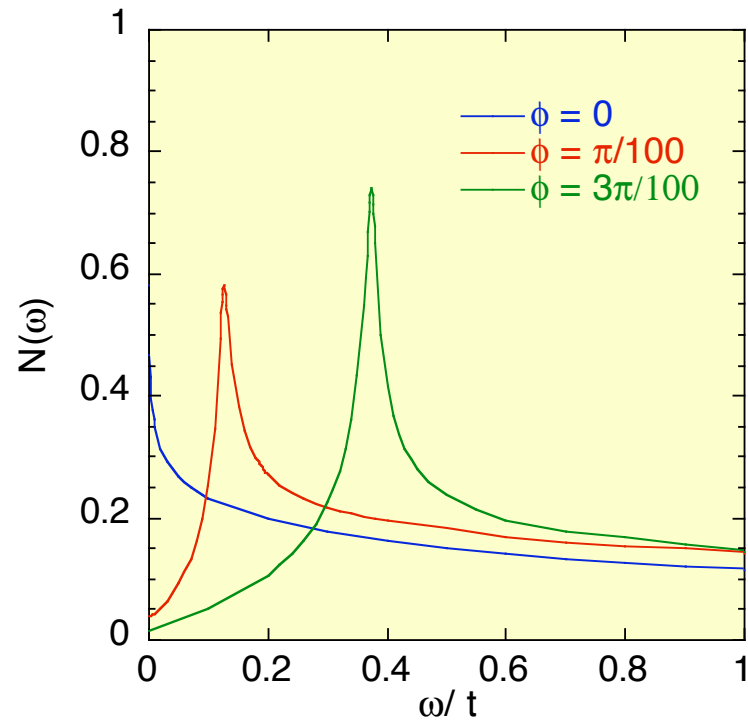
Density of states

$$N_\sigma(k, \varepsilon) = -\frac{1}{\pi} \text{Im} G_\sigma(k, \varepsilon + i\delta)$$

Eigenfunction $\varphi_{\sigma m}(r)$

$$H\varphi_{\sigma m}(r) = E_{\sigma m}\varphi_{\sigma m}(r)$$

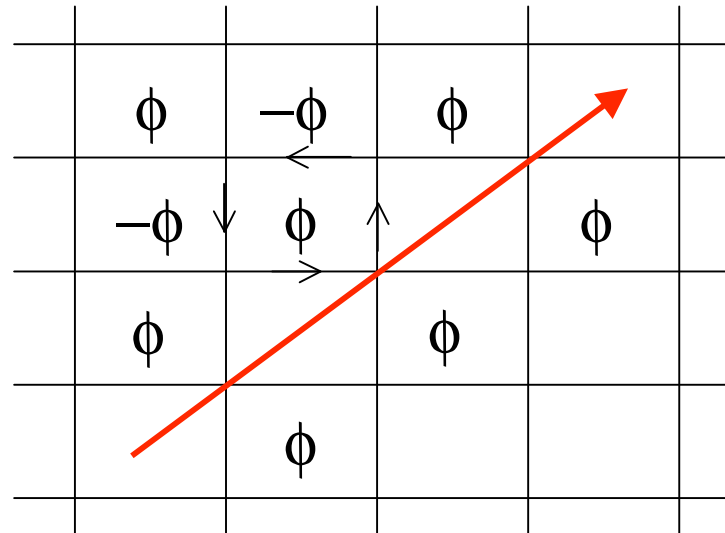
$$G_\sigma(r, r', i\omega) = \sum_m \frac{\varphi_{\sigma m}(r)\varphi_{\sigma m}^*(r')}{i\omega - E_{\sigma m}}$$



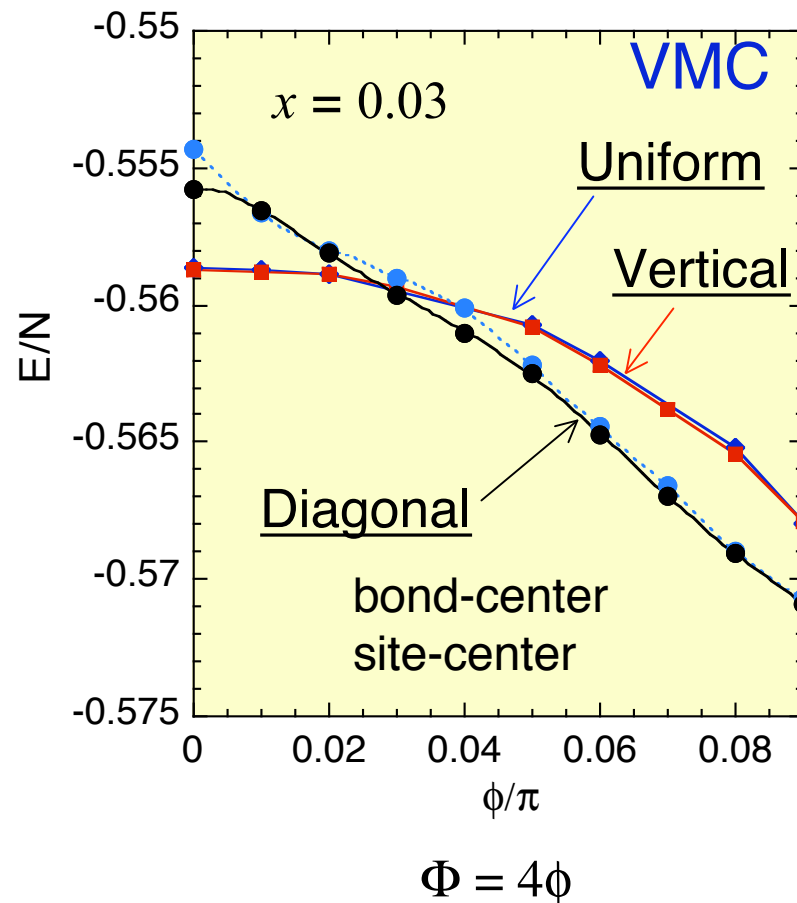
Diagonal stripes with Spin-orbit coupling

Spin-orbit coupling induces flux.

Spin-orbit coupling stabilizes the diagonal stripes.



Diagonal Stripe & d-density wave



T.Y. et al., Jmmm 272 (2004) 183.

d-density wave

d-density wave

$$i\Delta_Q Y(k) = \langle c_{k+Q\sigma}^+ c_{k\sigma} \rangle \quad Q = (\pi, \pi)$$

$$Y(k) = \cos(k_x) - \cos(k_y)$$

Nayak, Phys. Rev. B62, 4880 ('00)

Chakravarty et al., PRB63, 094503 ('01)

ϕ	$-\phi$	ϕ	$-\phi$
$-\phi$	ϕ	$-\phi$	ϕ
ϕ	$-\phi$	ϕ	
$-\phi$	ϕ		

Inhomogeneous density wave

$$i\Delta_Q Y(k) = \langle c_{k+Q\sigma}^+ c_{k\sigma} \rangle \quad \text{d-symmetry}$$

$$\Delta_{lQ_s\sigma} = \sum_k \langle c_{k+lQ_s\sigma}^+ c_{k\sigma} \rangle \quad \text{incommensurate}$$

$$Q_s = (\pi + 2\pi\delta, \pi) \quad \text{vertical}$$

$$Q_s = (\pi + 2\pi\delta, \pi + 2\pi\delta) \quad \text{diagonal}$$

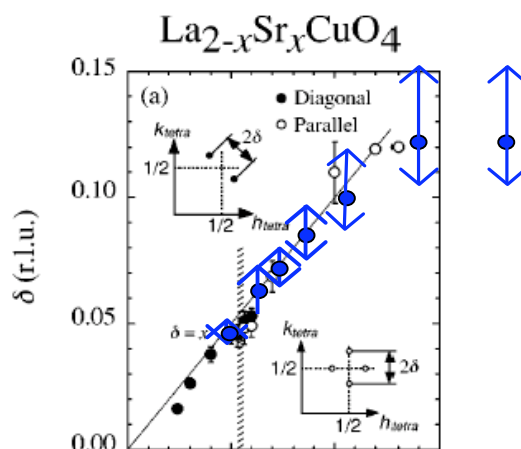
ϕ	$-\phi$	ϕ	$-\phi$
$-\phi$	ϕ	$-\phi$	ϕ
ϕ	$-\phi$	ϕ	
$-\phi$	ϕ		

8. Summary

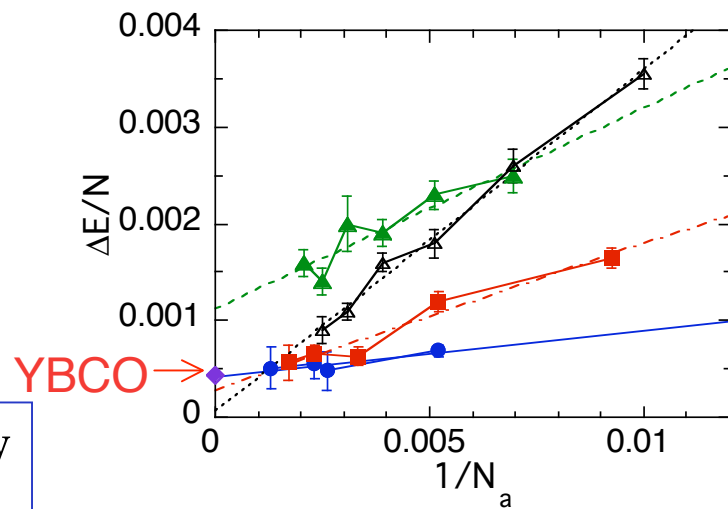
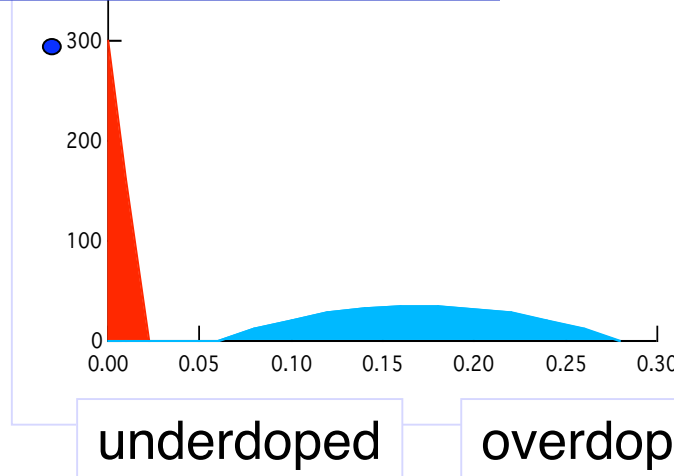
HTSC and Correlated Electrons

Variational Monte Carlo study of
BCS-Gutzwiller function

$$\Psi_{Cds} = P_G \prod_k (u_k + v_k c_{k\uparrow}^+ c_{-k\downarrow}^+) |0\rangle$$



Incommensurability
Neutron scatterings



Theoretical estimate of
SC condensation energy

Agreement with Exp.

$E_{\text{cond}} \sim 0.2 \text{ meV}$